Ecole Polytechnique
Master 1 – Sciences pour les défis de l'environnement
August 2016
OTALORA Marcia

RAPPORT DE STAGE DE RECHERCHE

SIMULATING THE SEINE RIVER DISCHARGE USING THE LAND SURFACE MODEL ORCHIDEE

Document non confidentiel

Option :	Environnement, Terre, Océan, Atmosphère
Directeur de l'option :	Thomas Dubos
Directeur de stage :	Agnès Ducharne
Dates du stage :	01 Mars au 15 Juillet
Adresse de l'organisme :	Université Pierre Marie Curie – UMR 7619 METIS UPMC Case 105 - 4 Place Jussieu 75252 Paris Cedex 05 France

Abstract

Land Surface Models (LSM) are potential tools that represent the exchanges happening at a soil-atmosphere interface and that are used to study the variability of water resources at a global and regional scale. Their application requires LSM to generate realistic simulations to represent the hydrological processes at different time scales. In this study we tested the LSM ORCHIDEE (ORganising Carbon and Hydrology In Dynamic EcosystEm) to simulate the Seine river streamflows (the amount of water going into a river) based on a 22-year simulation that was validated against the discharge observations of the hydrometric station Poses.

The purpose of this study was to improve the accuracy of the model simulations by analyzing four different atmospheric input datasets (forcings) and making different modifications on the model parameters related to the soil hydrology and vegetation dynamics. In the case of the forcings, the NCC and PGF forcings produced higher discharge values while the WFDEI and CRU-NCEP forcing showed initially a negative bias compared to the observations. Moreover, all the simulations presented a seasonality problem showing a delay of the hydrograph. This suggested that further analysis of the river routing scheme should be performed in order to assess this issue.

In addition, the most effective modifications were related to the activation of the STOMATE module, which simulates the processes of vegetation and carbon dynamics, the dynamic roughness, which assess the computation of aerodynamic resistance, and the increased vegetation extinction coefficient which is related to the vegetation cover. These changes decreased the total evaporation and increased the final discharge considerably. In contrast, the modification of the infiltration process by cancelling the sub grid scale parametrization improved the partitioning between surface runoff and drainage which led to a better seasonal behavior of the river discharge.

Even though we achieved our goal of improving the simulated discharge, the final simulations still presented a seasonality issue which may be addressed by working on the partitioning between the drainage and surface runoff, the retention of water in the soil and most likely the way the streamflows are modeled by the routing scheme.

Table of Contents

LIST OF FIGURES

LIST OF TABLES

I. INTRODUCTION

The exchanges between water and energy that take place at a surface-atmosphere interface are key factors in understanding the Earth's climate. The relationship between land surface and atmosphere is explained by the fact that if there is any change in the fluxes of heat and water from the land surface to the atmosphere, this would also represent a change in the humidity, temperature and air pressure in the atmosphere (Bonan 2006; Pitman 2003).

Land surface models (LSMs) were first introduced in atmospheric general circulation models (GCMs) to treat the exchanges happening at a soil-atmosphere interface which represented a major concern in the development of climate simulation (Haughton et al. 2016; Pitman 2003; Overgaard et al. 2005). Thanks to their development, LSMs are now considered to be a potential tool in the prediction of the variability and uncertainties of water resources at a regional scale which plays an important role in the planning and management of water resources and the impact of climate change which makes model validation a fundamental step in the development of these models (Overgaard et al. 2005; Gascoin et al. 2009; Decharme & Douville 2007; Gao et al. 2004; Ngo-Duc et al. 2005; Hurkmans et al. 2008).

Guimberteau et al. (2009); Materia et al. (2010) and Ngo-Duc et al. (2007a), between others, showed that the LSM model validation can be done by comparing the results for the variable river discharge against observations since it integrates all the large-scale hydrological processes on land surface and there is a considerable amount of river flow data, whereas other hydrological variables such as soil moisture or evaporation are poorly known.

The present study focuses on the simulation of the river discharge by the LSM ORCHIDEE (ORganising Carbon and Hydrology In Dynamic EcosystEm) on the Seine river basin, one of France's largest river basins. This basin covers about 78,600 km^2, including the Paris metropolitan area (Seine-Normady Water Agency 2002; GIP Seine-Aval 2013; Billen et al. 2009). Due to its high level of importance to the industrial, agricultural and overall French population, several studies have been carried out over the Seine basin to understand its mechanism and how it could be affected in different climatic and anthropogenic future scenarios (Ducharne et al. 2007; Rousset et al. 2004; Billen et al. 2009).

In this study, we tested the ability of the LSM ORCHIDEE to simulate the river discharge of the Seine basin, by comparing it to the observed data at the hydrological station Poses, which drains almost 80% of the whole Seine basin. To test the sensitivity of the model to different parameters, four atmospheric input datasets (forcing) differing in resolution were used. In addition to this, modifications on the model code and user defined parameters were also tested in order to achieve better results. Since ORCHIDEE is a model in development, the main objective of this study was to evaluate the performance of the model at a local scale in order to be able to identify the parameters have a bigger weight in the calibration of the model and finally improve the final simulated river discharge.

II. THE WATER BUDGET

This section is dedicated to introduce the main concepts relevant to this study.

The hydrological cycle is a complex system where the total amount of water on Earth does not change, but is always in movement, and it can be found in different states (solid, liquid, and gas), as show in Figure 1.

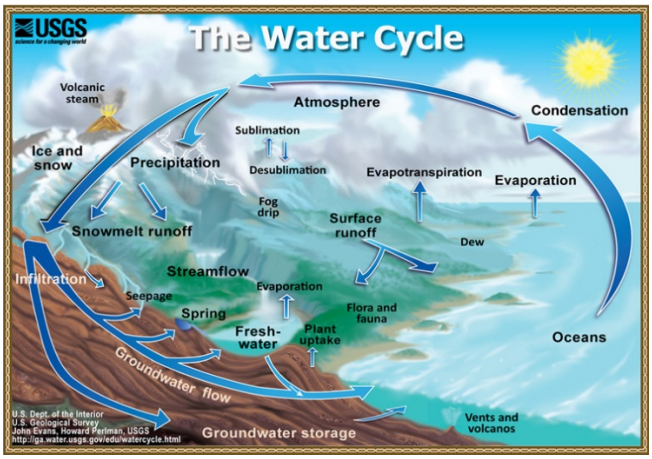

Figure 1. The water cycle. Published by U.S. Department of the Interior & Survey, 2016. Retrieved from http://water.usgs.gov/edu/watercycle.html

The major components of the global water cycle include the evaporation from the land and ocean surfaces, precipitation onto the ocean and land surfaces, the net atmospheric transport of water from land areas to ocean, and the return flow of water from the land back into the ocean. On land, the situation is considerably more complex, and includes the deposition of rain and snow on land; water flow in runoff; infiltration of water into the soil and groundwater; storage of water in soil, lakes and streams, and groundwater; polar and glacial ice; and use of water in vegetation and human activities (University of Illinois n.d.; U.S. Department of the Interior & Survey 2016; Dingman 2015).

The water budget is basically the difference between the input and the output of water and the changes in the storage through a region. In simple terms it can be described by equation *(1)*

$$I - O = \frac{dS}{dt} \qquad (1)$$

Where the instantaneous rate of input I minus the instantaneous rate of output O equals the instantaneous rate of storage S. In a drainage basin each portion of the budget is a specific process of the cycle (Dingman 2015). For any time period of length Δt the water balance equation can be expressed as equation *(2)*:

$$P + GW_{in} - (Q + ET + GW_{out}) = \Delta S \qquad (2)$$

where P is the precipitation (liquid and solid), GW_{in} is ground-water inflow, Q is stream outflow (liquid), GW_{out} is ground-water outflow and ΔS is the change in all forms of storage (liquid and solid) over the time period. ET is evapotranspiration, known as the total of all water that leaves a region as vapor via direct evaporation from surface-water bodies and ice, in addition to transpiration (water evaporated from vegetation). If we consider that the water storage is not

significantly increasing or decreasing over time, and because watersheds are topographically defined and ground-waterflow is driven by gravity, it is also assumed that ground water and watershed divides coincide so that GW_{in} is neglibible. Under these assumptions the water balance equation *(2*) can be writen as:

$$Q + GW_{out} = P - ET \qquad (3)$$

where the sum $Q + GW_{out}$, is also known as the total runoff.

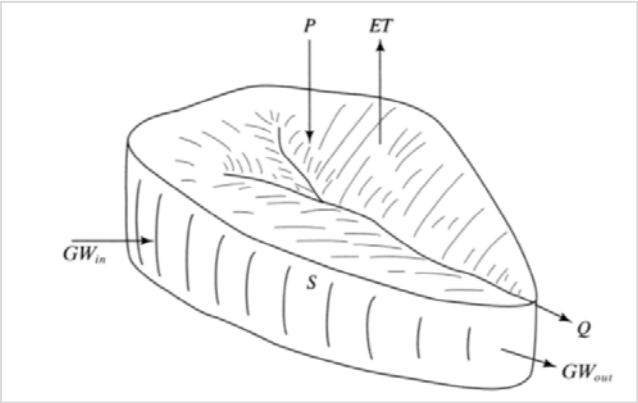

Figure 2. Schematic diagram showing the components of regional water balance in a water shed. Retrieved from (Dingman 2015, p.19)

III. METHODOLOGY

1. AREA OF STUDY: THE SEINE BASIN

The Seine is a 777-kilometer long river and an important commercial waterway within the Paris Basin in the north of France. It officially rises at Source-Seine, 30 kilometers northwest of Dijon in northeastern France in the Langres plateau, flowing through Paris and into the English Channel at Le Havre (Figure 3). Its main tributaries are the Oise, the Marne, the Yonne, the Eure, and the Aube rivers (Viennot et al. 2009; GIP Seine-Aval 2013) covering a total area of 78 600 km^2 or around 12% of the total French territory.

The land is relatively flat with altitudes generally under 500 meters, except in the Morvan massif. The climate is oceanic and temperate with an average annual rainfall of 745 millimeters (mm) and an average annual potential evapotranspiration of 759 mm. Annual rainfall varies between 300 and 1,300 mm depending on the area. The average monthly temperature in Paris is between 2.5°C (in January) and 24.6°C (in August). Periods of freezing temperatures are short along the coast in the west, but lengthen towards the eastern edge of the basin.

The sedimentary basin of the Seine is characterized by a complex hydrogeology, with many stacked aquifers and semipermeable layers. This type of geological structure contains numerous aquifers of extremely varying size and structure (alluvial, sedimentary and fractured aquifers) (Seine-Normady Water Agency 2002; Viennot et al. 2009). Most of the basin is situated over the Paris basin which is composed of sedimentary rock layers; the most important aquifers being found in the carbonate and detrital deposits. Rousset et al. (2004) explained that this configuration is responsible for the high underground water contribution the discharge, which reaches more than 80% of the Seine river flow in summertime and 40% in winter based on the modeling of the Seine river basin using the hydrogeological model MODCOU. In constrast for the Somme river basin, located in the north of France, the groundwater flow feeds around 90% of the total flow (Viennot et al. 2009).

Approximately 17.5 million people live over the total basin area, this makes the Seine river basin a subject of interest for scientists and researchers, as well as authorities which are involved in the natural resources management, specifically water management.

Table 1. Hydrological characteristics of the Seine basin – Adapted from Seine-Normady Water Agency (2002)

Surface area of the basin	78 600	Km^2
Annual precipitation	745	mm/year
Annual potential evapotranspiration	759	mm/year
Average discharge at Poses hydrometric station	538	m^3/s

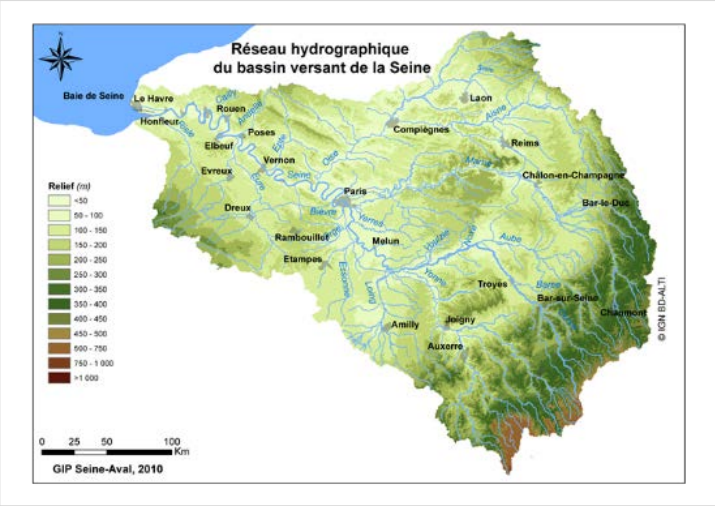

Figure 3. The Seine river basin. Retrieve from Seine-Normady Water Agency (2002)

2. THE ORCHIDEE MODEL

ORganizing Carbon and Hydrology In Dynamics EcosystEms (ORCHIDEE) is a Land Surface Model (LSM) developed by the Institut Pierre Simon Laplace (IPSL) with the objective to simulate the energy and water balance of terrestrial ecosystems (Krinner et al. 2005). The model can be run in a coupled set-up with a General Circulation Model (GCM) or on an "offline" mode as a stand-alone land surface model. In the case of an offline simulation the atmospheric conditions are provided by the 'forcing files', which need to provide information about the near-surface air temperature, humidity and wind speed, the precipitation and incoming radiation, and the surface atmospheric pressure. Running the model in offline mode gives the possibility to cover a global domain or a single grid point depending on the resolution of the forcing file.

ORCHIDEE is composed from three main modules: SECHIBA, STOMATE and LPJ, which can exchange information among them as represented in Figure 4, however only two of them were used during this study.

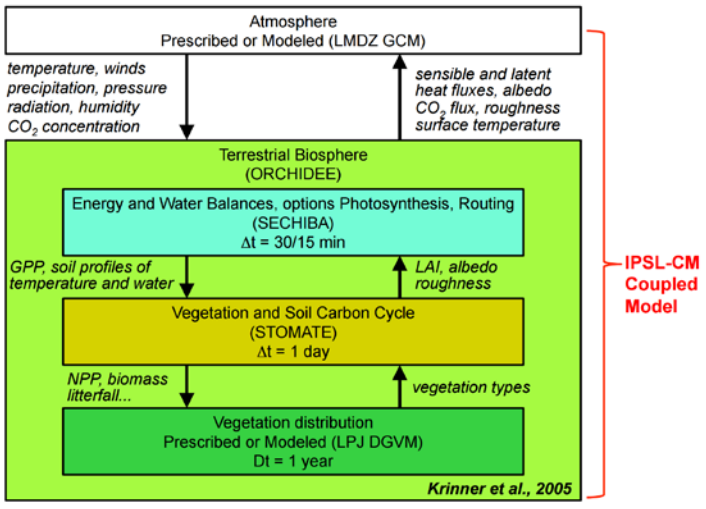

Figure 4. Graphic representation of the ORCHIDEE modules. Retrieved from http://labex.ipsl.fr/orchidee/index.php/about-orchidee

2.1. SECHIBA (Schématisation des Echanges Hydriques à l'Interface entre la Biosphère et l'Atmosphère)

Developed initially by Ducoudré, Laval, & Perrier (1993), this module is responsible of simulating the energy and water exchanges between the atmosphere, soil and vegetation. SECHIBA considers a time step of 30 minutes to represent these physical processes and in terms of spatial resolution, the size of each grid box is determined by the atmospheric 'forcing' files. The model conducts the simulation by considering one grid box at a time and considering the vertical processes and fluxes at each grid box. In addition, it considers each grid box to be covered by a mosaic of uniform vegetation tiles which properties come from a selection of 13 plant functional types (PFTs).

2.1.1. SOIL HYDROLOGY

The model works with two types of soil-hydrology schemes: one consisting of 2 layers based on the bucket model (Manabe 1969) and the second one considering 11 layers introduced by Rosnay & Polcher (2002). The downloadable version of ORCHIDEE assumes the latter as the standard scheme and it is the one used in this study.

The 11-layer scheme is based on a physical approach of the vertical distribution of water in unsaturated soil. The soil column is divided into 11 layers of increasing thickness with depth to solve the non-saturated vertical soil water flow otherwise known as the Richards equation (Richards 1931), assuming gravitational drainage at the bottom (Guimberteau et al. 2014). Under this approach, the volumetric water content (θ) is used to determine the soil water flow instead of the pressure head which is normally considered to solve Richards equation (Campoy et al. 2013). All variables are considered to be horizontally homogeneous, neglecting the lateral fluxes between adjacent grids.

Equation *(4)* shows the relationship between the vertical distribution of the water content (θ) and the flux field, where t is time (s), z is the soil depth below the surface (m), q the flux field (m s^{-1}), and s represents the transpiration ($m^3.m^{-3}.s^{-1}$) (Campoy et al. 2013; Guimberteau et al. 2014; Ducharne 2015).

$$\frac{\partial \theta(z,t)}{\partial t} = \frac{\partial q(z,t)}{\partial z} - s(z,t) \qquad (4)$$

An adaptation of Darcy's equation to unsaturated conditions is used to describe the vertical flux (Equation *(5)*. In ORCHIDEE the hydraulic conductivity and diffusivity are described by the Mualem (1976) and Van Genuchten (1980) formulation (Equation 6 and 7),

$$q(z,t) = -D_i\big(\theta(z,t)\big)\frac{\partial \theta(z,t)}{\partial t} + K\big(\theta(z,t)\big) \qquad (5)$$

$$K(\theta) = K_s\sqrt{\theta_f}\left(1 - \left(1 - \theta_f^{1/m}\right)^m\right)^2 \qquad (6)$$

$$D_i(\theta) = \frac{(1-m)K(\theta)}{m\alpha}\frac{1}{\theta - \theta_r}\theta_f^{-1/m}\left(\theta_f^{-1/m} - 1\right)^{-m} \qquad (7)$$

where D_i is the diffusivity ($m^2.s^{-1}$), K the hydraulic conductivity ($m.s^{-1}$), K_s the saturated hydraulic conductivity ($m.s^{-1}$), while α (m^{-1}) and m are parameters for the Van Genuchten-Mualem model. The dimensionless parameter m, is related to the classical parameter *n* of Van Genutchen by:

$$m = 1 - 1/n \tag{8}$$

Finally, the relative humidity is defined as the difference between θ_r the residual water content ($m^3.m^{-3}$), and θ_s the saturated water content ($m^3.m^{-3}$) as showed in equation (9).

$$\theta_f = \frac{\theta - \theta_r}{\theta_s - \theta_r} \tag{9}$$

$$K_s(z) = K_s^{CP} \min(1, e^{-\frac{z - z_{lim}}{z_s}}) \tag{10}$$

In order to solve these set of equations, ORCHIDEE considers the soil's characteristics through the parameters $K_s, \theta_r, \theta_s, m$ and α which are defined according to three types of soil texture classes (d'Orgeval et al., 2008), with values obtained from Carsel & Parrish (1988) Carsel and Parrish (1988). K_s is assumed to be constant within the first 30 cm from the surface, but it decreases exponentially going further down as showed in Equation (*(10)*), where K_s^{CP} is the saturated hydraulic conductivity from Carsel and Parrish (1988); $K_s(z)$ is the hydraulic conductivity at a (z) depth; z_s is the characteristic depth of exponential decay for K_s; and z_{lim} is 30 cm. To assure consistency among the parameters K_s, n and α are also modified with K_s based on a log-log regression introduced by d'Orgeval (2006) and d'Orgeval et al. (2008).

2.1.2. INFILTRATION, SURFACE RUNOFF AND DRAINAGE

With the 11 layer soil hydrology scheme, the precipitation rate and the soil hydraulic conductivity define the partitioning between soil infiltration and surface runoff production. The parametrization of infiltration into the soil is inspired by the model of Green and Ampt (1911), as explained by d'Orgeval (2006), with a sharp wetting front propagating like a piston. The infiltration process is described in the scientific documentation of ORCHIDEE (Ducharne 2015) as follow:

"A time-splitting procedure is used to describe the wetting front propagation during a time step as a function of its speed. To this end, the saturation of each soil layer is described iteratively from top to bottom. The time to saturate one layer depends on its water content, and on the infiltration rate from the above layer, which is saturated by construction (the top layer, with a 1-mm depth using the 11-mode discretization, is assumed to saturate instantaneously).

To simplify, the effect of soil suction is neglected, which leads to gravitational infiltration fluxes. The infiltration rate is equal to the hydraulic conductivity at the wetting front interface, called K_i^{int}, and defined as the arithmetic average of $K(\theta_i)$ in the unsaturated layer i reached by the wetting front and at the deepest saturated node $(i-1)$. "

Surface runoff is generated if the water flux available for infiltration is larger than K_i^{int}, defining an infiltration-excess runoff. In addition, a sub-grid distribution of infiltration is considered which has a reductive or increasing effect on the effective infiltration and surface runoff rate. To this end, the hydraulic conductivity is spatially distributed using an exponential probability density function, which defines fractions of the grid-cell where the local conductivity is smaller than the grid-cell mean K_i^{int}, thus enhancing surface runoff. Finally, partial re-infiltration is allowed in grid cells where the mean slope is small ≤0.5%, which acts in contrast to decrease surface runoff (D'Orgeval et al., 2008).

The second contribution to total runoff is free gravitational drainage at the bottom of the soil. It is equal to the hydraulic conductivity at the soil bottom, and thus depends on the corresponding water content (Equation 11):

$$Q_N = K(\theta_N) \quad (11)$$

2.1.3. EVAPOTRANSPIRATION

Evaporation from the land surface, along with precipitation, is a primary determinant of water availability in the global water cycle. It englobes the transfer of water from plants and soil to the atmosphere (transpiration, canopy evaporation or interception and soil evaporation) which influences water resources and runoff (Blyth et al. 2010). In the case of ORCHIDEE, previous evaluations of the model have noticed an overestimation of the bare soil evaporation, particularly during the winter season. This means a decrease in the water reservoirs for the following season, limiting evaporation in summer (Tootchi 2015).

In ORCHIDEE the total evaporation depends on the following conditions:

- **Aerodynamic resistance**, which controls the transfer heat and water vapor from the surface into the air above the canopy layer. It depends on the roughness length of the surface which is a boundary condition and the wind speed.
- **Surface temperature**, which is used in the calculation of saturated surface specific humidity in the soil evaporation formulation.
- **Air specific humidity**, which is the ratio of the total mass of water vapor to the total mass of air in each grid box and that is related to the vapor pressure exerted by the water molecules at a specific time.
- **Leaf Area Index (LAI),** a greater coverage of vegetation means a less percentage of bare soil and a higher interception by vegetation and transpiration.
- **Soil moisture**, the evaporation from soil depends on the availability of water in the soil to evaporate, thus the difference between the wet and dry seasons.

2.1.4. THE ROUTING MODULE

The routing module is in charge of transforming the total runoff calculated in each grid cell into streamflow in the river network, which will be finally discharged from the continents (land) into the oceans. The routing plays an important role in the conversion of the simulated runoff into river discharge as showed by Marengo et al. (1994) and Ducharne et al. (2003), however this

is not addressed in this study. In the case of ORCHIDEE the routing model considers three linear reservoirs: stream, fast and slow as seen in Figure 5.

The routing scheme of ORCHIDEE works currently input data at a 0.5º resolution, including the flow direction (based on the map of Vorosmarty et al., 2000), map of river basins, and the topographic index controlling the flow velocity. It is possible to define sub basins if ORCHIDEE is run at a coarser resolution (defined by the resolution of the atmospheric forcing files). Water flows in 8 possible directions and have three possible outlets: lake inflow, coastal flow and river flow.

The water is routed into each grid cell and divided into the three reservoirs, each with different residence time. As shown in Figure 5, the slow reservoir is fed by the drainage and flows out to the stream reservoir of the next grid cell; the fast reservoir receives the surface runoff from the previous grid cell and flows to the stream reservoir of the next grid cell; the stream reservoir represents the rivers, and it flows to the next stream reservoir.

The flow from each reservoir depends on a reservoir property (g_i) which is constant for each reservoir, and a topographic index (*k*), which is included in the input file the module reads. The reservoir property does not vary horizontally but distinguishes the three reservoirs, while *k* characterizes the impact of topography on travel time in each sub-basin, and is assumed to be the same in the three reservoirs of a given grid cell, even though it derives from stream-routing principles introduced by Ducharne et al. (2003). This travel time is thus assumed to be proportional to stream length in the sub-basin, and inversely proportional to the square root of stream slope (Ngo-Duc et al. 2007b).

The water balance within each reservoir is computed using the following continuity equation:

$$\frac{dV_i}{dt} = Q_i^{in} - Q_i^{out} \quad (12)$$

$$Q_i = \frac{V_i}{\tau_i} \quad (13)$$

$$\tau = k \cdot g_i \quad (14)$$

where V_i (kg) is the water amount in the reservoir i considered ($i = 1,2,3$), Q_i^{in} and Q_i^{out} represent the incoming and outgoing flow respectively.

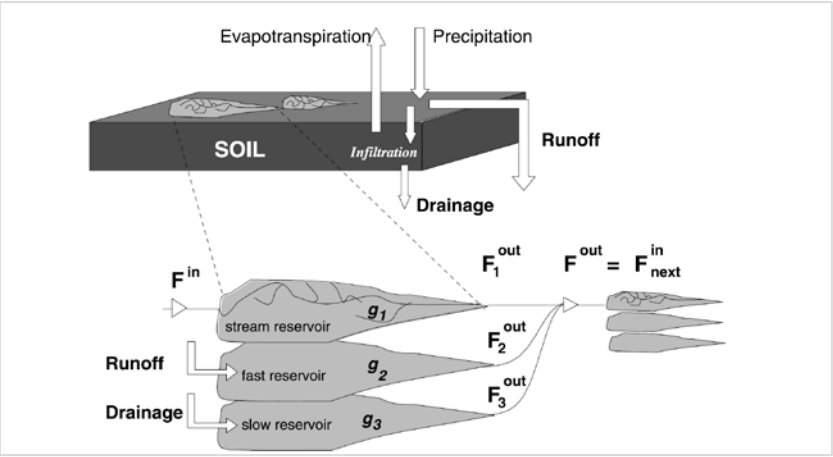

Figure 5. Transfer scheme from the routing model in ORCHIDEE. Retrieved from Ngo-Duc et al. (2007b)

2.2. STOMATE

The STOMATE module was developed Nicolas Viovy in 1996, and it is in charge of simulating the soil carbon cycle, providing the carbon flow within the soil-plant-atmosphere continuum (G. Krinner et al. 2005). The carbon dynamics and phenology are simulated considering the processes of photosynthesis, soil carbon dynamics, respiration and vegetation growth. In each grid cell, up to 12 plant functional types (PFTs) can be represented simultaneously, in addition to bare soil. It is modulated by the leaf area index (LAI) growth, specific to each PFT represented in the model. LAI dynamics (from carbohydrate allocation) is simulated by STOMATE which models the allocation of assimilates, autotrophic respiration components, foliar development, mortality and litter and soil organic matter decomposition.

The STOMATE module can be omitted or activated by the user if desired. In the first case, the phenology of the vegetation needs to be prescribed, owing to monthly LAI (Leaf Area Index) maps. During this work, STOMATE was initially not activated to prevent from potentially complex interactions between soil moisture and vegetation development. Nonetheless, it was further taken into consideration in order to observe if the vegetation exchanges with the land and atmosphere played an important role in the area of study.

2.3. LPJ

The LPJ (Lund Postdam Jena) module was developed by Sitch et al. in 2003. It works at a large scale basis representing the terrestrial vegetation dynamics, meaning the evolution of the vegetation considering the soil biogeochemistry, the physiology and the dynamics of the vegetation, the climate conditions, and the competition among the PFTs. The LPJ module works at a longer time step than SECHIBA or STOMATE, normally considering 1 year per time step.

3. COMPONENTS OF A SIMULATION IN ORCHIDEE

ORCHIDEE model requires a number of datasets in order to perform a simulation. In addition, certain specifications are also asked to the user in order to define limits that are required by the model. In this section we explain the components that were part of the simulations we performed.

3.1. BOUNDARY FILES IN ORCHIDEE

3.1.1. ATMOSPHERIC FORCING

Running the model in an “offline” version requires the input of the meteorological variables considered for the energy-water balance. An atmospheric forcing file is a data set of reanalysis estimates combined with gridded data sets from observations. The accuracy and reliability of these data sets remains questionable and represent a major challenge for the estimation of the land surface water budget, which is a crucial part of climate change prediction (Ngo-Duc et al. 2005; Decharme & Douville 2006). Each forcing represents a method of reanalysis and set of observations, consequently it is logical to assume that there will be a natural sensitivity to their use which is explained in the results section IV.1. Table 2 details the forcing datasets used.

Table 2. Atmospheric forcing data sets tested in the Seine river simulations

Name	**NCC**	**WFDEI**	**PRINCETON (PGF)**	**CRU-NCEP**
Time Step	6 hours	3 hours	3 hours	6 hours
Spatial resolution	1° × 1°.	0.5° x 0.5°	1° × 1°.	0.5° x 0.5°
Time period available	1948 to 2000	1979 to 2014	1948-2008	1948-2002
Reference	Ngo-Duc et al. (2005)	Weedon et al. (2014)	Sheffield et al. (2006).	Provided by Nicolas Viovy: nicolas.viovy@lsce.ipsl.fr

3.1.2. SOIL TEXTURE MAP

The soil texture map is related to the value of saturated hydraulic conductivity Ks. ORCHIDEE reads by default the soil texture from the Zobler (1986) texture map at 1° resolution. The Zobler texture classes go from 0 to 7, however they are reduced to only three final soil textures: Coarse, Medium and Fine soil which respectively correspond to the sandy loam, loam, and clay loam USDA texture classes. The values of the corresponding hydrodynamic parameters are extracted from the values of Carsel and Parrish (1988). Each grid cell is assigned with only one soil texture class based on the largest fraction of the 3 final soil textures.

3.1.3. PLANT FUNCTIONAL TYPE MAP (PFT)

ORCHIDEE considers a global map of vegetation cover of a resolution of 5km x 5km to define the fraction of the vegetation type for each grid cell. This map, product of the Coupled Model Intercomparison Project Phase 5 (CMIP5), is a historical vegetation map combined with the Olson ecosystem classification (Olson et al., 1983). 13 final Plant Functional Types (PFT) are selected base on the method of the dominant vegetation, the first being the bare soil. Finally, the number of soil columns is reduced to a maximum of three: one gathering every forest PFT, one for every PFT with grass and crops, and one for the bare soil PFT and the “nobio” surface types, such as ice, free water, cities, etc.

3.1.4. LEAF AREA INDEX MAP

When the dynamic vegetation module (STOMATE) is not activated, ORCHIDEE requires an LAI map tailored for the 13 PFTs (Plant Functional Types) considered by the model. Two maps were tested in this study, both products of the STOMATE module of ORCHIDEE and one of them defined as the default option for the simulations. The default map is based on the “Tag1.6” of ORCHIDEE (dating of 2006), but it is unclear how exactly these two maps were constructed. This test was aimed to show the impact of the LAI on the simulation, but due to the unavailability of further information regarding the origins of these maps, only one forcing was tested, in this case the PGF forcing.

3.1.5. ROUTING

As explain in Section III.2.3., the routing is based on the topographic index, basins and flow directions which are all contained in the file map “routing.nc” that is available for the ORCHIDEE user. It is necessary nonetheless to establish a time step for the routing scheme, for which we assumed the default time step of one day or 86400 seconds.

3.2. USER DEFINED PARAMETERS

ORCHIDEE offers the possibility to change a number of parameters that control certain conditions in each module. In this study, we focused on the some of the parameters related to the soil hydrology and vegetation related parameters.

3.2.1. Precipitation Spread (SPRED_PREC)

This parameter refers to the way the precipitation is distributed over time within the forcing time step. The standard value considers the precipitation to be distributed over half of the forcing time step. This means that for a 3-hourly forcing (i.e. WFDEI) the precipitation would be distributed uniformly over 3 ORCHIDEE time steps (3x30min) when SPRED_PREC=3, or over 6 ORCHIDEE times steps (6x30min) if SPRED_PREC=6. On the other hand, if SPRED_PREC=1, then it is assumed that all the precipitation is distributed over the first ORCHIDEE time step within the 3-hourly forcing time step (first 30 min). This has a direct impact on the infiltration and creation of surface runoff.

3.2.2. Van Genuchten parameters (A0, A_POWER, N0, N_POWER)

These values are used in the Van Genuchten-Mualem model seen in section III.2.1.1. . They correspond to the values α and *n*, which are obtained from the Carsel and Parrish (1988) table according to the hydraulic conductivity and soil texture.

3.2.3. Soil hydraulic conductivity (Ks) and root infiltration capacity (Ks_fact)

This makes reference to the saturated hydraulic conductivity (Ks) which following d'Orgeval (2006, p81-82) and d'Orgeval et al. (2008, section 2.1.3), decreases exponentially below the top 30 centimeters and it is related to the soil texture and a decay factor. The standard decay rate value is 2.0. In addition to the decrease of Ks, the presence of roots in the first layers is a multiplicative factor of the Ks towards the surface. This value is controlled by Ks_fact which standard value is 10.

3.2.4. Vegetation Extinction Coefficient (VEGET_FRAC)

This value is related to the amount of net radiation reaching the soil surface in function of the Leaf Area Index as proposed by the Monsi & Seaki relationship (1953) which says that light attenuation in the canopy was approximated by Beer's Law. The higher the value of VEGET_FRAC, the more light is intercept by the upper canopy and therefore the higher the photosynthesis depending on the LAI.

3.2.5. Dynamic roughness (R_DYN)

The roughness length is a boundary condition in the calculation of the aerodynamic resistance, which mostly dependent on roughness length of the surface and wind speed. The activation of the dynamic roughness leads to a variation of the roughness length (z0 parameter) with the LAI. The inclusion of the Su formula (Su et al. 2001) for z0 leads to reduce the bias on latent heat flux at winter for deciduous forest (Tootchi 2015).

3.3. MODIFICATIONS IN THE SOIL HYDROLOGY MODULE CODE

In addition to the user defined parameters it is also possible to make changes directly to the code of the modules. Three modifications on the module that controls the soil hydrology processes were tested and are described as following:

- **Corrected water stress**: This change in the code was included automatically within an update (new revision) of the model. The way in which the water stress was calculated was modified in order to increase the amount of infiltration and reduce the surface runoff. This function varies between the wilting point and field capacity, before it was considered to be a square root function that reached the “no stress” limit from a certain value of volumetric water content and generated a higher surface runoff. It was modified to a linear function eliminating the dependence on the amount of water available resulting in a higher rate of infiltration.
- **Modified Sub-grid Infiltration**: This change was done manually in the ORCHIDEE code and aimed to reduce the surface runoff by eliminating the sub grid infiltration which was originally based on an exponential probability distribution (Section 2.1.1). With the No sub grid infiltration option, the mean rate at which the water infiltrates to the soil depends strictly on the hydraulic conductivity, and is therefore higher that in the original version. As result, surface runoff gets reduced.
- **Uniform Ks**: this version includes the above change (Modified sub grid infiltration) but in addition the infiltration front propagation is limited by the saturated hydraulic conductivity (Ks) only, instead of the average hydraulic conductivity of Ks and the conductivity of the unsaturated soil layer reached by the infiltration front. By increasing the hydraulic conductivity considered for the infiltration process, this change should further increase the infiltration and decrease the surface runoff.

4. SIMULATION DESIGN

4.1. SIMULATION DOMAIN AND PERIOD

To perform a simulation in an “offline” version of ORCHIDEE it is necessary to define the spatial domain and time period of the simulation. Figure 6 shows the Seine river basin map in two spatial resolution. The coordinates that define the Seine river basin domain were 45.0° N, -1.0° E and 51.0° N, 6.0° E and in terms of the time scale, the years considered correspond to a period of 22 years in total, from 01/01/1979 to 12/31/2000.

4.2. INITIALIZATION

For any new simulation the model starts to run considering “empty” reservoirs which, depending on the characteristics of the area of study, will require a certain number of iterations before they reach a steady state, this is known as a “spin-up”. In our case, two years were considered enough to reach a steady state after analyzing the fluctuation of the main reservoirs such as soil moisture over the whole time period of study, thus the final analysis considered the period from 01/01/1981 to 31/12/2000.

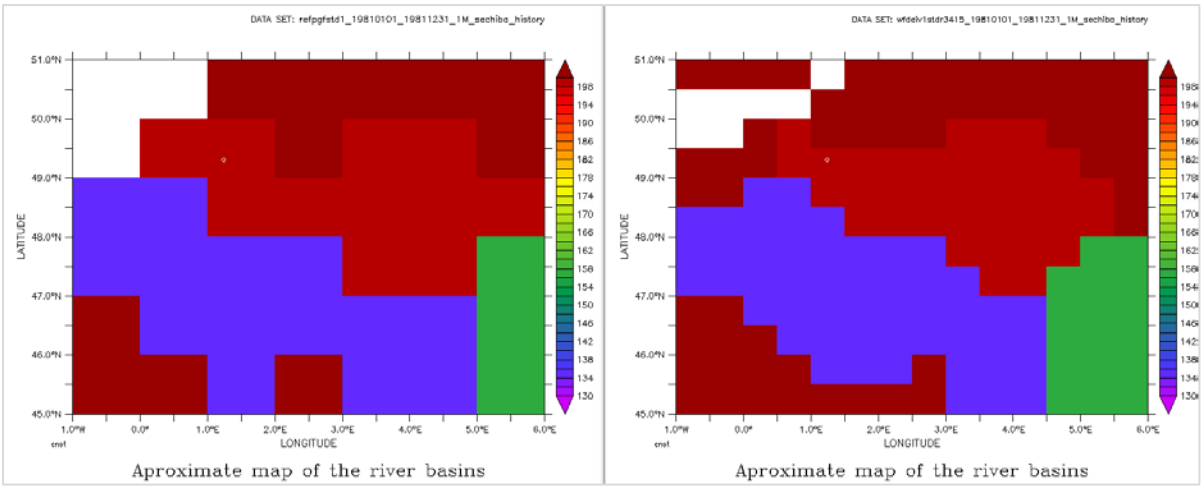

Figure 6. Seine river basin map (in light red) at the two horizontal resolution used in this study: 1.0° (left) and 0.5° (left). The Poses station is represented by the white circle with coordinates 1.23º E, 49.3º N.

5. VALIDATION

5.1. OBSERVATION DATA

In order to validate the results, observed data from the hydrometric station Poses, located at the coordinates 1.23º E, 49.3º N (Figure 6), was obtained from the French hydrometric service (Banque Hydro). This station covers a sub-basin of 64939 km^2, which represents almost 80% of the whole Seine river basin and it is the most downstream hydrometric station before entering the Seine estuary, in which the tidal activity of the ocean influences the river flow. It is a heavily monitored station, with a coverage of 91 % over the years of analysis (1981 to 2000) and a pluri annual monthly average of 527.9 m^3/s. Figure 7 shows the daily discharge fluctuation over the time period considered.

In order to reduce the bias that could arise by the missing data at Poses station, an adjustment to the simulation results was also made by replacing the simulated data by “no data” in the case there were no available observations.

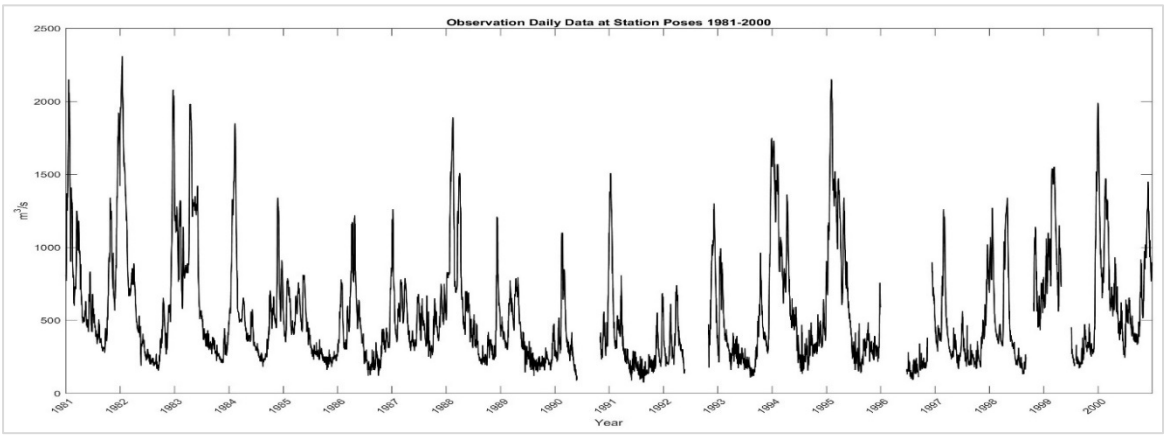

Figure 7. Daily data observation data at Poses Station

5.2. NASH SUTCLIFFE EFFICIENCY *(E)*

The evaluation of hydrologic model behavior and performance is commonly made through comparisons between simulated and measured streamflow at the catchment outlet. Efficiency criteria is used by hydrologists to provide an objective assessment of the "closeness" of the simulated behavior to the observed measurements (Krause & Boyle 2005; Gupta et al. 2009).

The efficiency *E* proposed by Nash and Sutcliffe (1970) is defined as one minus the sum of the absolute squared differences between the predicted and observed values normalized by the variance of the observed values during the period under investigation. It is calculated as:

$$E = 1 - \frac{\sum_{i=1}^{n}(O_i - P_i)^2}{\sum_{i=1}^{n}(O_i - \bar{O})^2} \qquad (15)$$

with O observed and P predicted values. The range of E lies between 1.0 (perfect fit) and $-\infty$. An efficiency of lower than zero indicates that the mean value of the observed time series would have been a better predictor than the model. Similar to the coefficient of determination r^2, the Nash-Sutcliffe is not very sensitive to systematic model over- or under prediction especially during low flow periods.

IV. RESULTS

The summary of the simulations tested is showed in Annexe A. Each of them represented a test with different modifications of parameters.

1. INFLUENCE OF THE FORCING

In this section, the sensitivity of the model to the four forcing files presented above is discussed. Figure 8 shows the results obtained for four simulations with the same characteristics with the exception of the forcing file. The variables selected for the analysis are those that were considered to be representative of the energy-water exchange processes at the surface-atmosphere interface, still, the model provides a significant range of additional variables that were not considered in this analysis.

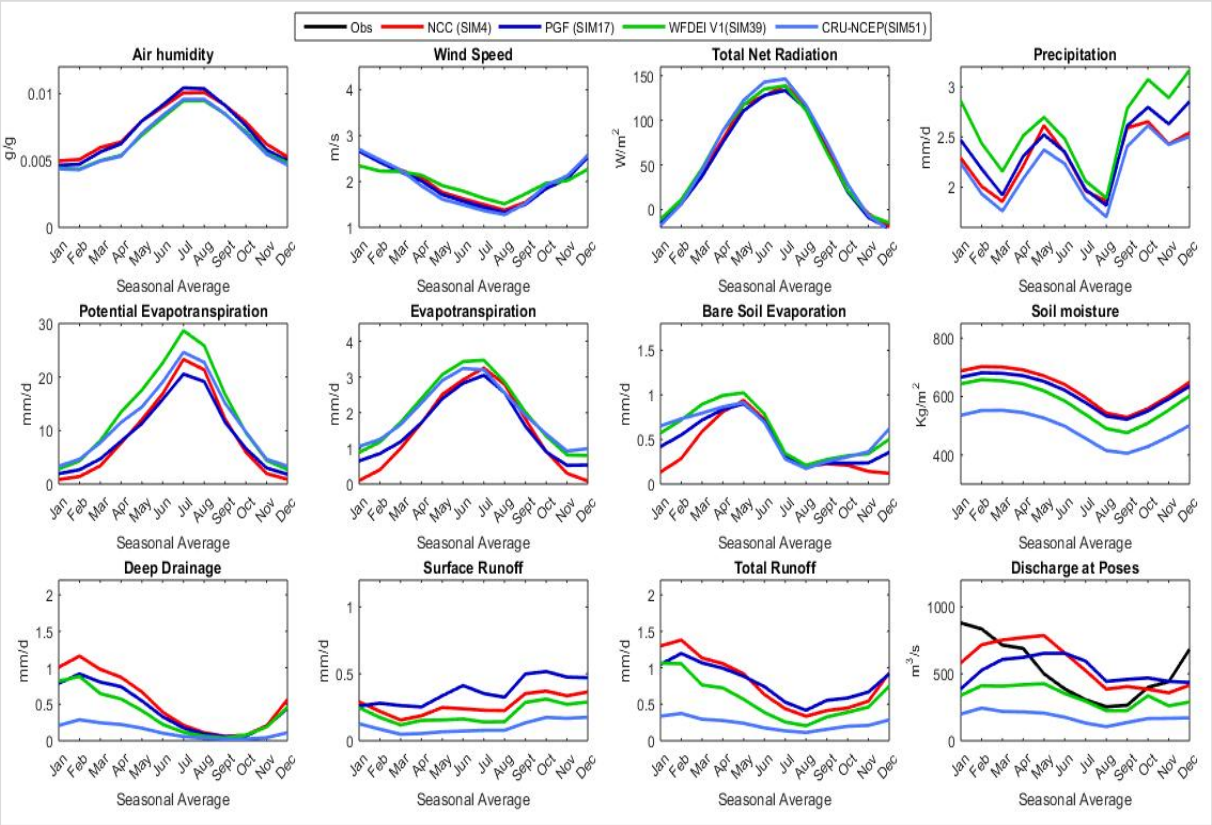

Figure 8. Pluriannual (1981-2000) mean monthly average of selected variables for four different forcing files under standard conditions of ORCHIDEE, NCC (SIM 4), PGF (SIM 17), WFDEI (SIM 39), and CRU-NCEP (SIM 51). Spatial averages over the Seine basin (see Figure 6), except for the river discharge at Poses.

Each forcing has undergone a different process of data assimilation and correction, therefore there are visible differences in the precipitation, wind speed as well as in the air humidity and net radiation inputs. Notoriously, the most striking difference induced by the forcing is the mean river discharge (Annexe B) with a factor 3 between the lowest mean discharge (with CRU-NCEP), which also show a strong underestimation compared to the observed discharge, and the highest one (with NCC). In addition, WFDEI (Sim 39) and CRU-NCEP (Sim 51) do not

show a seasonal contrast unlike the other forcings, showing mild variations over the twelve months due to the low discharge volume that is generated.

In Figure 9 we compare the maximum, minimum and mean discharge between the observation data and the simulations. Noticeably, WFDEI and CRU-NCEP underestimate the river discharge in all three scenarios. Distinctively, NCC and PGF did not show a defined tendency, showing better results for the minimum values but not a defined trend for the mean and maximum values. The underestimation of the maximum discharge is related to the bad seasonality of the simulation, which is also supported by the fact that some of the minimum discharge values are overestimated, particularly for the PGF forcing.

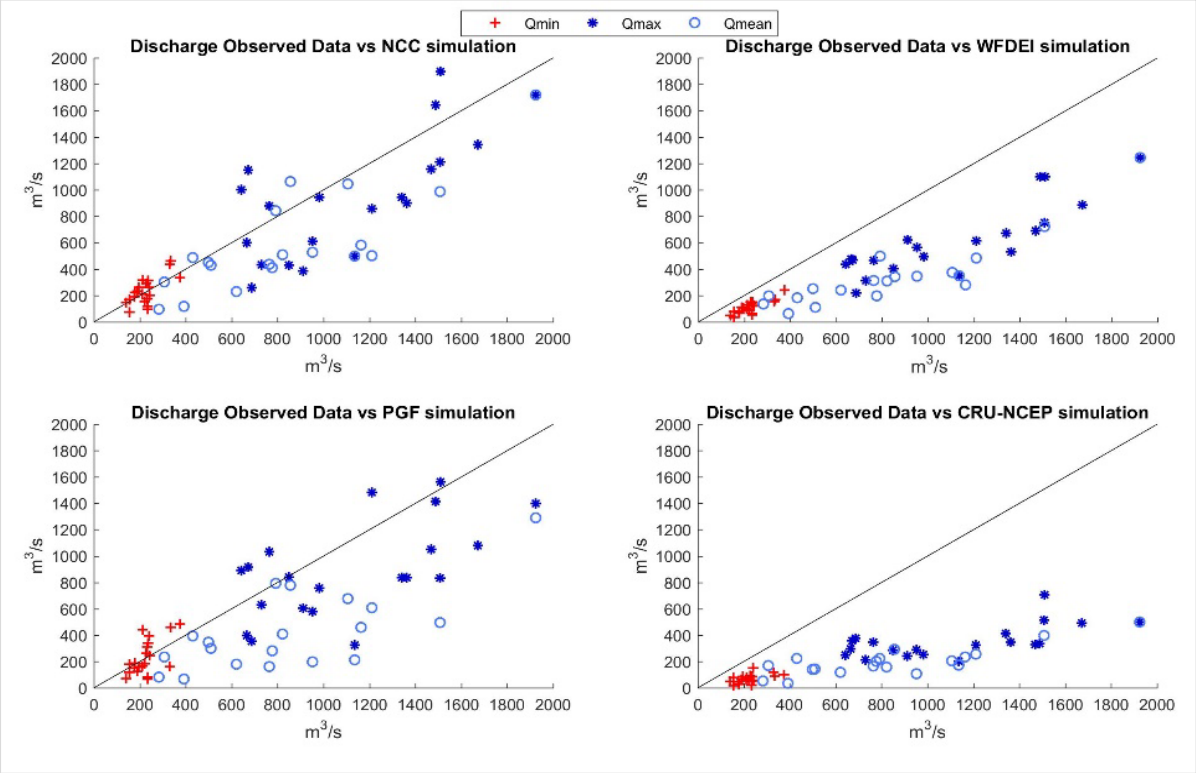

Figure 9. Comparison between observation (x-axis) and simulation discharge (y-axis) at Poses station, considering the annual mean of the maximum (Qmax), minimum (Qmin) and mean discharge (Qmean) for each of the 20 years (1981-2000) of study.

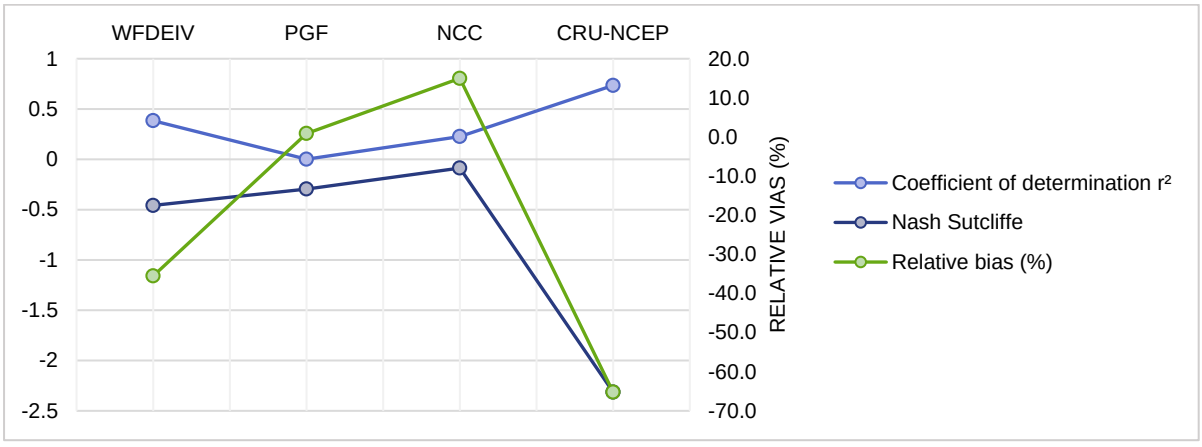

Figure 10. Performance criteria results - Comparison between forcing under standard conditions

In terms of total amount of precipitation, WFDEI presented the maximum rate with 2.58 mm/d of combined rainfall and snow, followed by PGF (2.37 mm/d), NCC (2.28 mm/d) and ultimately CRU-NCEP (2.18 mm/d). Despite having the highest precipitation input, WDFEI did not lead to the highest discharge, with an annual average of 332 m^3/s, compared to PGF with 524 m^3/s and NCC with 561 m^3/s under the same simulation conditions. This can be explained by the influence of a combination of factors which include the air humidity, wind speed and total net radiation. In the case of WFDEI, even though it showed the highest precipitation, the low air humidity, combined with a higher wind speed and total net radiation, lead to a higher potential evapotranspiration during the months of March to September which has an effect on the generated discharge. CRU-NCEP, besides having a low precipitation (2.18 mm/day), showed a higher total net radiation (60.38 W/m^2) and lower air humidity (0,00659 g/g) which added up to a higher potential evapotranspiration than the NCC and PGF forcings, however in comparison to the WFDEI it is the wind speed difference that results in a lower potential evapotranspiration for CRU-NCEP.

The influence of wind speed over the potential evapotranspiration is linked to the aerodynamic resistance that takes place on the border between the air flow and the surface. A higher wind speed near the surface is equal to a higher turbulent diffusion which increases the evapotranspiration from the soil due to a lower aerodynamic resistance (more chances for the water particles to leave the soil into the atmosphere). On the other hand, air humidity is also considered as a driving factor of evapotranspiration. Lower values imply a higher evaporation from the soil whereas higher values of air humidity will decrease the evaporation rate. As evaporation proceeds, the surrounding air becomes gradually saturated and the process will slow down and might stop if the wet air is not transferred to the atmosphere. Finally, the total net radiation is related to the energy that is required to change the state of the molecules of water from liquid to vapor and it is strongly related to the energy balance; a higher value of total net radiation increases the energy available for evaporation.

Furthermore, the precipitation and total evaporation also have a direct impact over the total runoff, which is the amount of water that is considered by the routing scheme of the model and that is linked to the discharge. Figure 10 shows that PGF and NCC both produced the highest discharge which is proportional to the total runoff, however there is a visible difference during the winter season which is explained by the bare soil evaporation. NCC presents a lower bare soil evaporation rate during winter, this is caused by a higher air humidity for the same period, which means a lower rate of evaporation and a higher availability of water destined to the routing reservoirs, particularly during the months of January to April. In comparison to the other forcings, NCC shows a closer simulation discharge to the observation for this period however the seasonality is still not the same as the observed data.
A crucial aspect considered during the evaluation of an LSM is the seasonal variation of the simulated results compared to the observations. It is evident that in the case of the simulations ran over the Seine basin, there is a lag between the simulated discharge and the observations of several months. This could be related to the routing scheme which can delay the river discharge compared to the total runoff based on how the river flow is modelled. In the case of

the Seine, Gomez (2002) estimated that the time between a uniform precipitation pulse and the resulting peak river discharge at the outlet takes around 10 to 15 days. In our case, if we compare the total runoff to the river discharge there is a difference of one month which is considered to be too high for a watershed of this size. This suggests that working with the routing scheme can correct this lag, however this work was focused on the water budget and runoff production processes since it is necessary to estimate the correct amount of volume discharge before working with the river flow modelling.

Figure 10 shows a summary of the performance criteria for each of the simulations. In this case, CRU-CNEP has the highest r^2 (0.74) although it showed an underestimation with a negative bias of -65%. WFDEI also showed a negative bias of -35.5% and a relatively low r^2 of 0.38. NCC concluded with a bias of +15% but with a r^2 of only 0.23, similarly the PGF forcing only produced an overestimation of 0.9% but with the worst r^2 within the forcings (0.15). Under the Nash Sutcliffe scope, values for all simulations were not promising reaching negative values in all cases suggesting that the results were far from optimal.
In order to answer the question regarding which is the correct forcing to use with ORCHIDEE, it is not possible to be based only on the efficiency parameters for one simulation, further validations tests would be required such as the comparison of latent flux data which were not included in this study. The main focus was to improve the simulation with each one of the forcings in order to achieve more realistic results by changing certain parameters related to the processes of soil evaporation.

2. INFLUENCE OF MODIFIED PARAMETERS RELATED TO VEGETATION

As described in section III.3, different components of a simulation can be modified by the user. In this case we grouped the parameters related to the modelling of vegetation in order to study the impact of them over the simulated discharge. The parameters related to the vegetation are:

- VEGETATION EXTINCTION COEFFICIENT (EXT_COEFF_VEG) Section III.3.2.4
- DYNAMIC ROUGHNESS (R_DYN) Section III.3.2.5
- STOMATE MODULE Section III. 2.2

We tested the effect of these parameters individually and then we proceeded to make possible combinations that could improve our results. Figure 11 shows the results for a simulation performed using the WFDEI forcing and Table 3 details the combinations made with the matching simulation number. The effect in the performance criteria parameters over each forcing is showed in Figure 12 .

Table 3. Detail of combinations considered for the analysis of the influence of the parameters related to vegetation. Each combination correspond to a simulation number depending on the forcing.

COMBINATION		NCC	PGF	WFDEI	CRU-NCEP	VEGETATION EXTINCTION COEFFICIENT	DYNAMIC ROUGHNESS	STOMATE MODULE
A		SIM 2	SIM 13	SIM 38	-	0.5	NO	NO
B		SIM 4	SIM 17	SIM 39	SIM 51	1.0	NO	NO
C		-	SIM 22	SIM 40	-	1.0	NO	YES
D		SIM 6	SIM 19	SIM 41	SIM 53	1.0	YES	NO
E		SIM 5	SIM 18	SIM 45	SIM 52	0.5	YES	NO
F		SIM 8	SIM 21	SIM 46	SIM 54	1.0	YES	YES

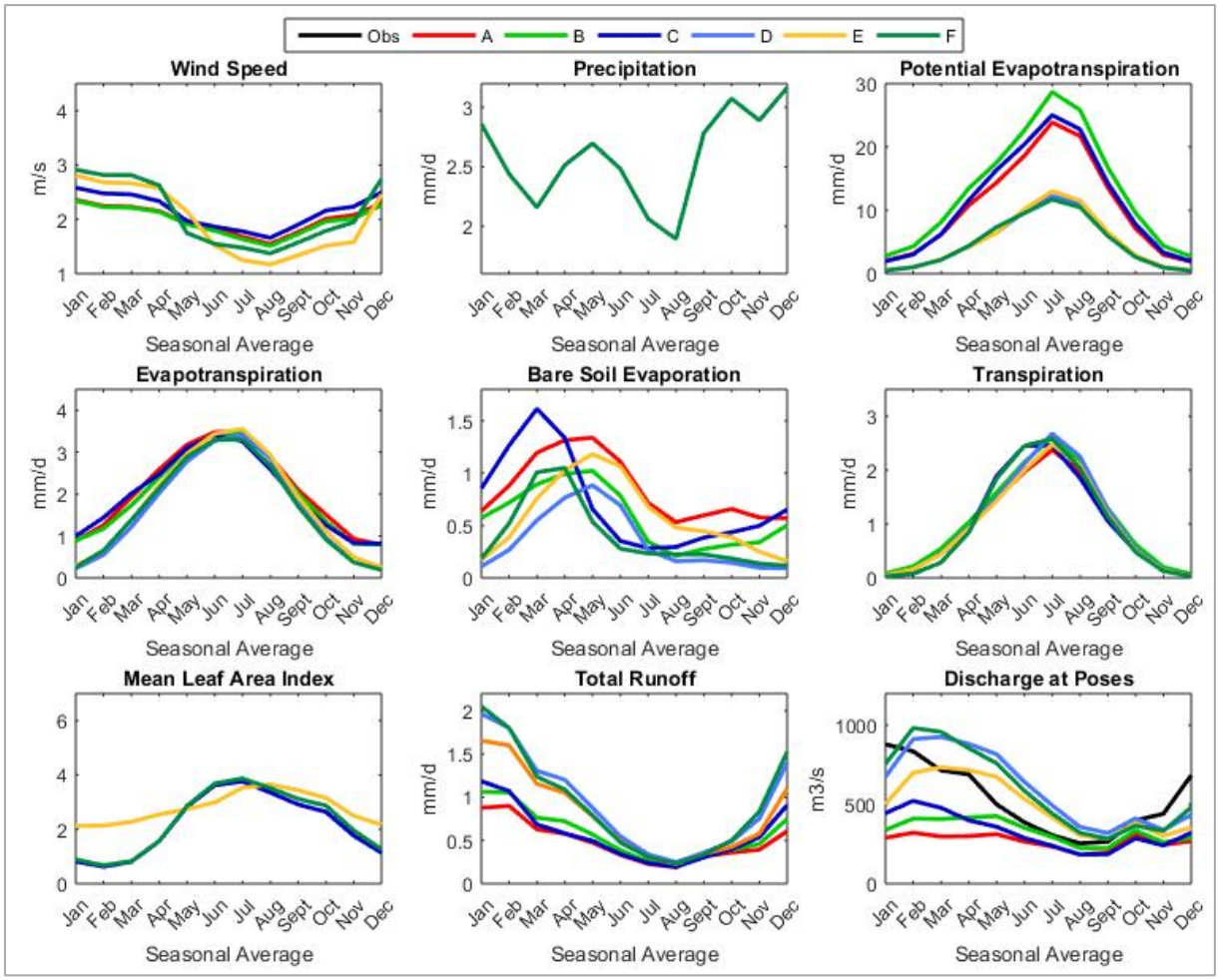

Figure 11. Pluriannual (1981-2000) mean monthly average of selected variables using the WFDEI forcing to show the effect of the modifications of parameters related to vegetation. The spatial averages over the Seine basin (see Figure 6), except for the river discharge at Poses.

One of the most noticeable changes regards the distribution of the wind speed at 2m caused by the activation of the dynamic roughness (R_DYN). The dynamic roughness changes the calculation of the wind speed by changing the roughness length z0 which later takes part in the aerodynamic resistance at 2m. It is also a function of vegetation and therefore it is affected when the STOMATE module is activated, as seen when comparing D and F or B and C.

The dynamic roughness induces a significant reduction in the potential evapotranspiration. In addition, this has an impact over the magnitude of the bare soil evaporation, which it is noticeably reduced due to a lower z0. Moreover, the change in the seasonal behavior is related to the activation of the STOMATE module and the extinction coefficient vegetation factor (EXT_COEFF_VEG). The activation of STOMATE produces a dynamic LAI that changes according to the season (summer/winter), thus there is a direct effect over the bare soil fraction and bare soil evaporation due to the way the vegetation phenology fluctuation. The Bare Soil Evaporation is a variable which is also linked to the extinction coefficient vegetation factor (EXT_COEFF_VEG). A higher extinction coefficient implies to a higher coverage of vegetation or less percentage direct radiation over the bare soil which reduces the total evaporation.

This relationship between the vegetation and the main variables involved in the water and energy balance affect the other three forcings in a similar way. The results are included in Annex C.

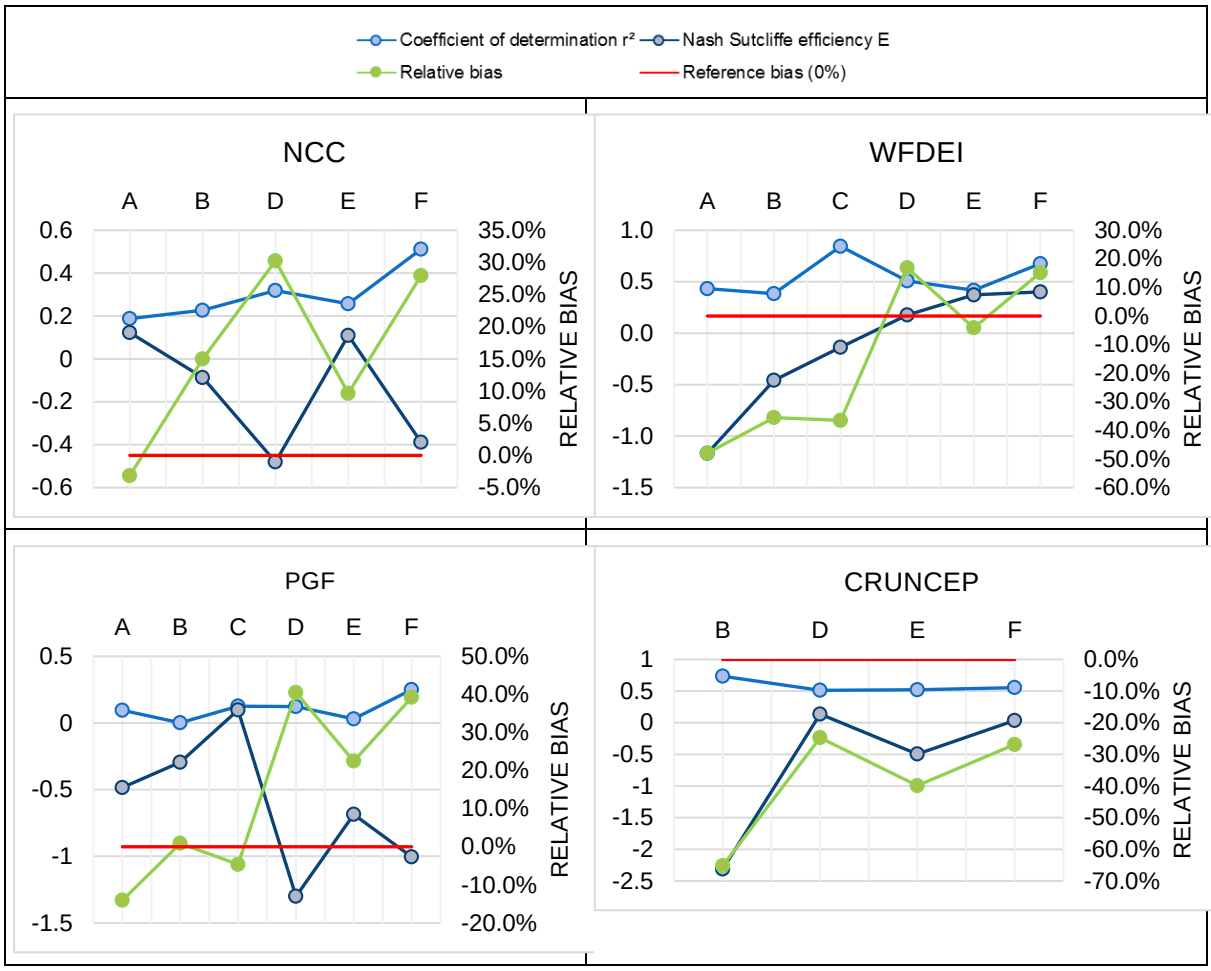

Figure 12. Performance criteria for the simulations with modifications related to the vegetation.

Figure 12, shows a summary of the results of the performance criteria for each of the forcing. WFDEI shows a gradual improvement of the Nash parameter as well as the coefficient of determination (r^2). Regarding the bias, WFDEI improved considerably from very high negative values of almost 50 % to a positive value of around 15%. PGF, on the contrary, showed a low coefficient of determination with no significant change between simulations. On the contrary, the overestimation of the discharge increased the bias and consequently the Nash efficiency also reached lower values. Initially the NCC forcing showed a better Nash value than the other forcings, however the increment of the bias also had a negative effect on the Nash value. This may be explained by its seasonal variation, as the discharge increases in volume the seasonality variation becomes less comparable to the observations.

CRU-NCEP showed no significant change in terms of the coefficient of determination. Its seasonal variation acts similarly to the observations which explains the higher r^2. Nevertheless, it is the lack of water which is the main problem with this forcing and this is reflected in the low values of the Nash parameter. In this case, the Nash efficiency parameter

showed considerable improvement despite the fact that it did not reach a value that could be considered as a “good” simulation (around 0.7).

3. EFFECT OF THE LAI MAP

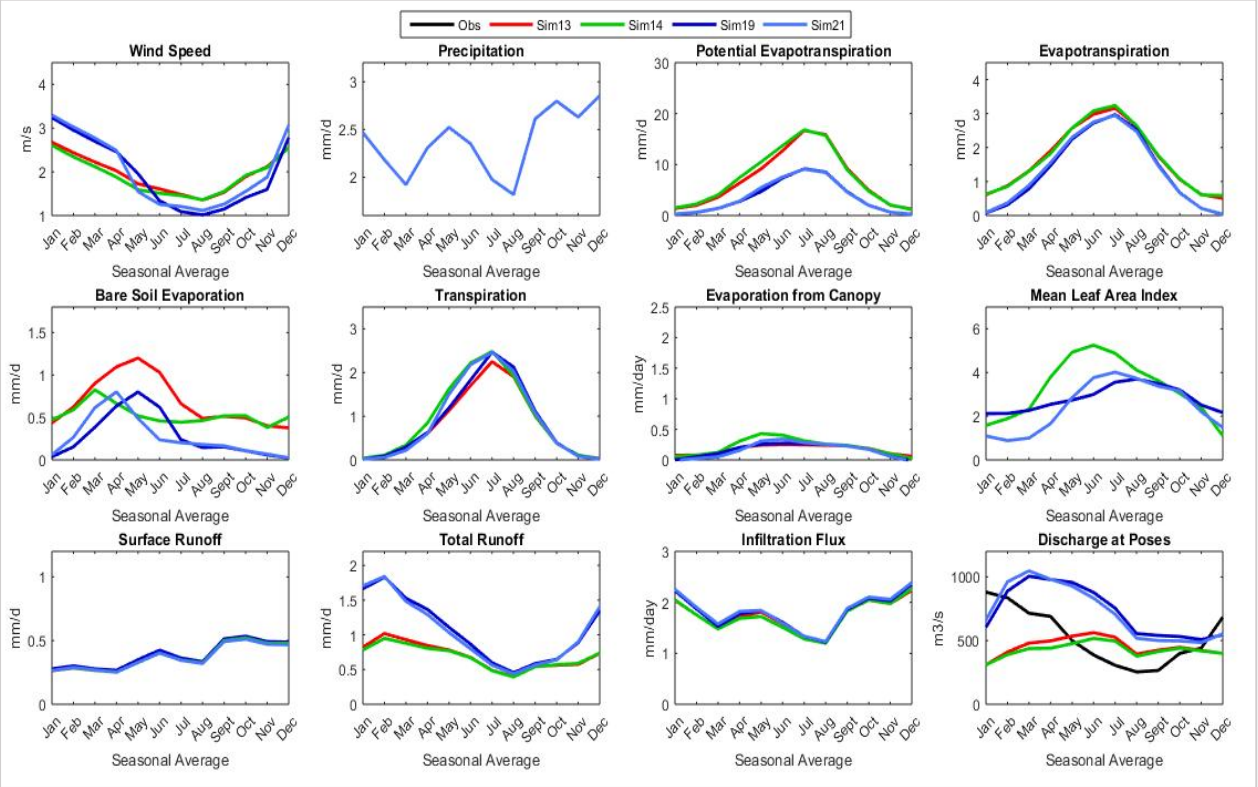

Figure 13. Pluriannual (1981-2000) mean monthly average of selected variables using the PGF forcing to show the effect of the LAI map. The lines are graphed in ascending order.

Figure 13 shows the main variables that could be influenced by the LAI map (Sim13 and Sim14) and the difference between using a standard LAI map and the activation of the STOMATE module (Sim19 and Sim21). The mean LAI suggests that the alternative map (green line) could be a product of a simulation using the STOMATE module, since they show a similar seasonal variation. However, if we consider only this change it does not have a positive impact on the total discharge produced. The alternative LAI map induces higher values than the LAI obtained with the standard map and than the LAI produced when STOMATE is activated. As a result, the alternative LAI decreases the bare soil fraction considerably compared to the Standard LAI, but as mentioned before, the alternative LAI has a different seasonality, leading the bare soil evaporation to peak during the month of March, and then decreases until the end of July. As a result, total evapotranspiration increases slightly, and there is a decrease in the final discharge.

We compared this effect to the one of STOMATE, but including the dynamic roughness and the higher extinction coefficient (Sim19 and Sim21). In these conditions, STOMATE (Sim21) produced a mean LAI with lower values than the ones with both LAI maps, except between May and August, when the LAI produced by STOMATE is higher than the one from the standard map. The smaller LAI produced with STOMATE than with the standard map, explains the increase of river discharge during the first months of the year, which better matches the

observation data. Yet, the sensitivity of the river discharge to the studied LAI changes is very small against the effect of the dynamic roughness and higher extinction coefficient.

Since the alternative LAI map did not have a positive effect on the simulation as it is showed by Figure 14, and since there was not sufficient information regarding its origin, we decided not to consider it in further simulations.

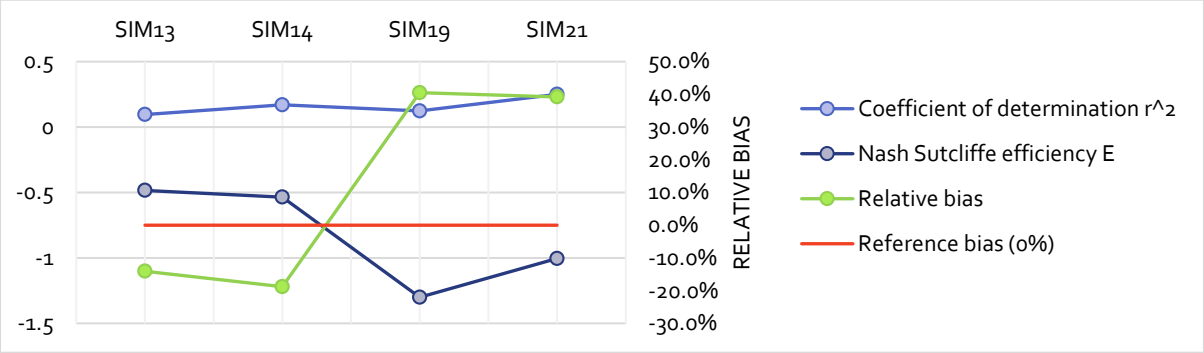

Figure 14. LAI map effect on efficiency parameters. Forcing: PGF

4. INFLUENCE OF THE MODIFICATIONS RELATED TO THE SOIL HYDROLOGY

In addition to the modifications made to the vegetation related parameters, one advantage that ORCHIDEE offers is the possibility to make modifications to the variables involved in the water balance, specifically the soil hydrology. We particularly focused on changes aimed at reducing surface runoff and/or increasing drainage. In this case, these modifications and their effects are portrayed using the forcing WFDEI. Once they were tested, the most effective modifications were selected for further combinations in order to get the best possible fit of the observed river discharge.

Figure *15* and Figure 16 show the results of the modifications that were tested; in both SIM 28 is the simulation considered as Standard based on the WFDEI forcing.

- Van Genuchten-Mualem Model (Figure 15 –SIM32): The modifications made here implied a change in the factors (α) and (*n*) which are involved in the Van Genuchten relationships solved for the total amount of water content and that are related to the inverse of air entry suction and the pore-size distribution. The change in the alpha and n factors induced an increment in drainage explained by the changes in the water retention, K, and resulting in a decrease in Soil Moisture. K decreases, the soil becomes less saturated and therefore hold less water which explains why the soil moisture is lower. The higher drainage provides a higher input towards the reservoirs and as a result there is a slight increase in the final discharge.
- Precipitation Spread (Figure 15 –SIM33; SIM34): The way the precipitation is distributed over a forcing time step has an impact in the volume of water that is infiltrated in the soil and the superficial runoff. A smaller “spread” of the precipitation means that the same input of water is distributed over a smaller sub-period within the

forcing time step, resulting in higher rainfall rates during the sub-period. As can be seen by Sim33 (SPRED_PREC=1), there is a direct effect on the infiltration flux and on the complement, which leaves the grid-cell as surface runoff. Within a smaller "spread" (Sim33), the soil does not have enough capacity to infiltrate the total volume of water and therefore a high percentage of water goes to the runoff. Even though this modification creates an overall increase in the final discharge, it also has an effect on the seasonal variation of the discharge, overestimating the surface runoff which results in a less coherent seasonality with the observations.

On the contrary, Sim34 considers a uniform distribution during the forcing time step (SPRED_PREC=6), this gives additional time for the soil to absorb and infiltrate the water from the precipitation as reflected by the higher soil moisture seen in Figure *15*. In this case, the surface runoff decreases as well as the total runoff, which is related to an increase of evapotranspiration by means of water conservation. Besides, the uniform spread of precipitation smooths the seasonal behavior of the discharge, which is related to the higher proportion of drainage/total runoff.

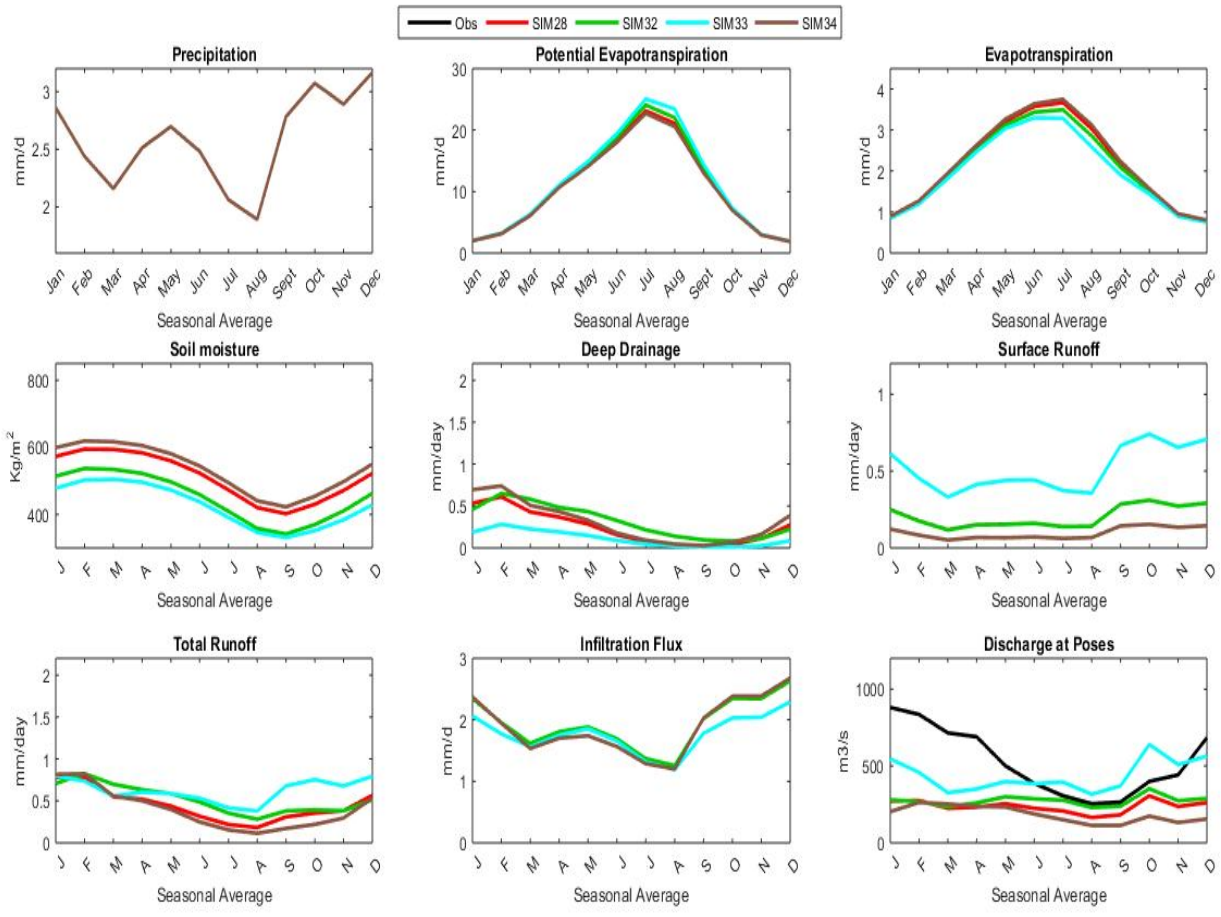

Figure 15. Pluriannual (1981-2000) mean monthly average showing the effect of the modifications of Van Genuchten parameters (SIM32) and the precipitation spread (SIM33 = SPRED_PREC 1 and SIM34 = SPRED_PREC 6) over the WFDEI forcing. The lines are graphed in ascending order.

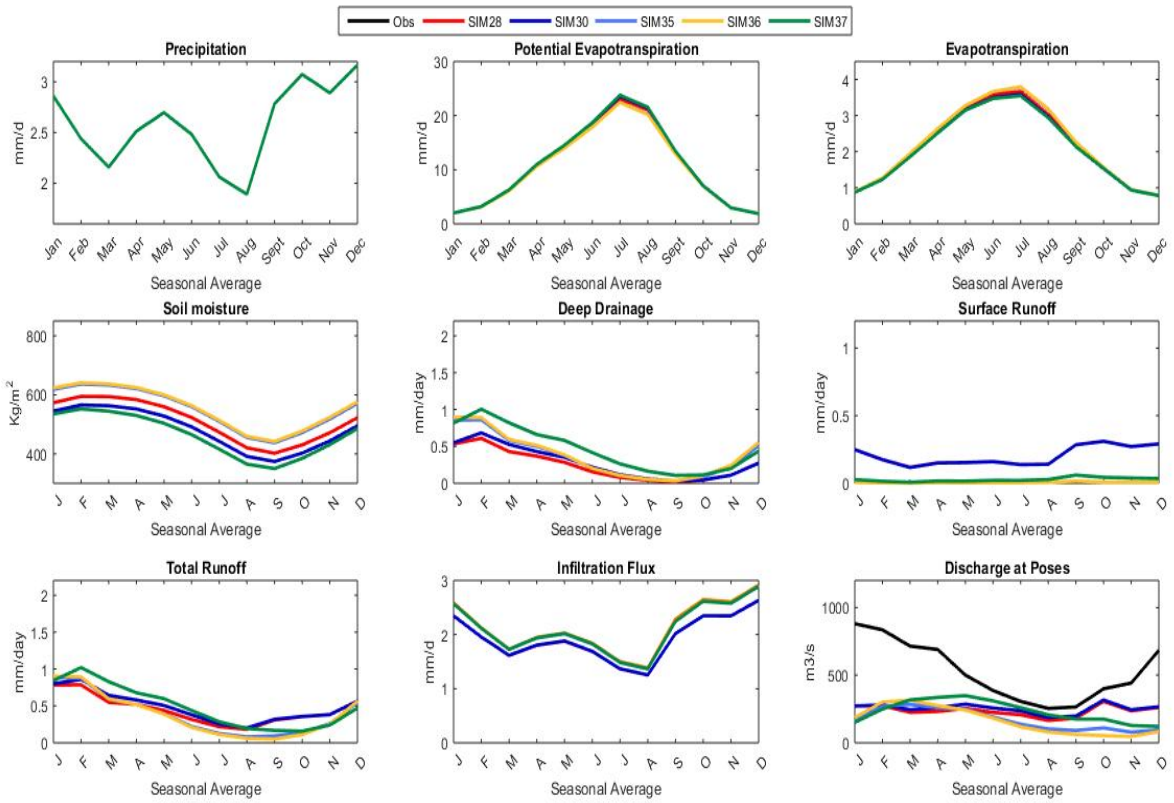

Figure 16. Pluriannual (1981-2000) mean monthly average showing the effect of the modifications of the modified decay rate of Ks (SIM30), the modified sub grid infiltration (SIM35), the uniform Ks (SIM36) and the combined modified decay rate and sub grid infiltration (SIM37) over the WFDEI forcing. The lines are graphed in ascending order.

- Modified Saturated Hydraulic Conductivity (Ks) and decay rate (Figure 16-SIM30): ORCHIDEE considers by default a Ks that decreases exponentially below the first 30 cm of soil. The modifications that were done suggest that Ks should undergo a slower rate of decay compared to the standard value and therefore allowing a higher drainage ultimately contributing to the discharge and total runoff. In regards of the multiplying factor (K_max), increasing its value was expected to increase the infiltration capacity and therefore provide a higher availability of water to the reservoirs for the routing scheme. As seen in Figure 16 (Sim30), this modification did not have a considerable effect on the final discharge. In fact, only a minimum change in the total runoff was observed compared to other modifications (Annexe B).
- Modified Sub Grid Infiltration (Figure 16-SIM35): As explained in section III.3, this modification was aimed to reduce surface runoff to increase infiltration and drainage by modifying the infiltration scheme by eliminating the exponential probability distribution and making it uniformly spatially distributed. As a result, the soil moisture increased to a higher percentage in comparison to the standard simulation and it also contributed to the decrease of the surface runoff. Moreover, the increase of drainage during the first months induced to a higher discharge within the months of February, March and April. However, as a counter effect, it reduces the discharge in the fall season. This is probably because surface runoff is a large contributor to the total runoff

in the fall, in this case the reduction to the surface runoff can be considered as too high (drainage/total runoff relation of 95%).

- Uniform Ks (Figure 16-SIM36): Similarly, the modification to the hydraulic conductivity, which includes the change in the sub grid infiltration as well, increases the discharge during the first couple of months, nonetheless its contrary effect in the end of summer and fall shows a slight increment than in the previous modification. This suggests that the surface runoff is strongly related to the Ks which may be improved by the incorporation of other surface runoff production mechanisms such as the one used in the TOPMODEL approach where the surface runoff is more dependent to the soil moisture.
- Modified Sub Grid Infiltration + Modified Ks (Figure 16-SIM37): The combination of both of these changes gave positive results by increasing the drainage and the total runoff which had an impact on the produced discharge, however it also produced a bigger lag compared to the observations, decreasing the discharge during the months of September to December instead of having an increasing tendency.

This overview of the influence of the modifications related to the hydrology module in ORCHIDEE, helped us during the decision making of the changes that should be considered during the following tests and that were later combined with other modifications in order to achieve the most realistic simulations. The final selection of simulations is described in the following section.

5. SELECTION OF FINAL SIMULATIONS

Based on combinations of the most effective changes (Table 4) a final selection was made to identify the best simulation for each forcing. Figure 18 shows the performance criteria obtained for the final simulations.

Figure 17 shows that these simulations all lead to an increased discharge compared to the control simulation (in red), which is true with all the forcings. As mentioned before, one of the most effective changes was the activation of the dynamic roughness which change in the calculation of the wind speed and induced a change in the aerodynamic resistance ultimately reducing the potential evapotranspiration. The combined effect with the modification of the vegetation extinction coefficient resulted in the most effective change regarding the volume discharge. This effect is enhanced by the activation of STOMATE, which provides the model with a dynamic vegetation cycle and therefore it helps to reach a better seasonal variation. The effect of the changes is most noticeable in the WFDEI and CRU-NCEP forcing (combination F), almost tripling the discharge within the first month but maintaining lower values for the months of September to December. Both forcing showed the highest negative bias (Figure 18) and very low Nash values for the control simulation (combination 0).

For NCC, combination F increases the discharge during the months of January to August but in a smaller scale than for the other forcings. This is explained by the fact that NCC has a higher discharge in the control simulation compared to the other forcing as a result of a higher

air humidity for the same period which concludes with a lower evapotranspiration; any change is therefore less noticeable for this forcing.

On the other hand, PGF had initially a lower bias compared with other forcings but it presented a problem with the seasonality, showing results that were too wet during the dry months and a lag of several months for the low flows. With combination F (including STOMATE, the dynamic roughness, and the increased extinction coefficient), this issue is partly handled. In terms of the efficiency of the simulations, PGF has Nash values that are the worst within all the forcing. This is due to the overestimation of the discharge, nonetheless the correlation between the simulation and observed data has improved with the different combinations that were tested.

Finally, CRU-NCEP was also strongly influenced by the combination of dynamic roughness and vegetation fraction and STOMATE. Although it showed initially the strongest negative bias (-65%), the combination of STOMATE with these parameters decreased the bias to -20%, still presenting a good correlation with the observed data.

The addition of the SUB GRID INFILTRATION modification is not as significant as the previous ones. As expected, it increased the discharge during the first months however there was an issue during the months of September to November. During this period the observations increased at a faster rate which is linked to the increasing precipitation, while the changes in combination G resulted in the smoothing of the discharge curve, so the lowest value is reached during the month of October. In terms of the efficiency, these changes had a minimal result in term of the correlation, and a negative effect for the Nash parameter in all the simulations.

In the case of the modification in the spread of precipitation (combination H), its effect is more important on PGF forcing than on the WFDEI forcing, as shown by the Nash value and r^2 in Figure 18. For these two 3-hourly forcings, combination H results in a more uniform spread of the precipitation, leading to a decrease in surface runoff, thus of total runoff. This is related to the correction process for precipitation that the forcing has undergone by, and this explains why its effect differs with each type of forcing. As for NCC and CRU-NCEP, there is no difference between the Sim3 and Sim4 because the forcing time step is 6 hours meaning that is equivalent to 6 times the ORCHIDEE time step, therefore they remain exempt by this modification.

At last, the inclusion of the modification in the Sub grid infiltration and Van Genuchten parameters showed a similar effect for all the forcings. These changes basically delay the hydrographs (mean seasonal cycles of river discharge) by about 1 month, which is contrary to the tendency of the observations and this is reflected in the coefficient of determination and the Nash parameter which show a negative effect with this change. This combination also produces an increase in the total discharge, which deteriorates the bias for all forcings but CRU-NCEP.

Table 4. Details of final selection of simulations in reference to Figure 17

COMBINATION		NCC	PGF	WFDEI	CRU-NCEP	VEGETATION EXTINCT COEFFICIENT	DYNAMIC ROUGHNESS	STOMATE MODULE	MODIFIED SUBGRID INGFILT	PRECIPITATION SPREAD	DECAY FACTOR AND VAN GENUCHTEN VALUES
0		SIM 1	SIM 11	SIM 28	SIM 51	0.5	NO	NO	NO	STD	NO
F		SIM 7	SIM 21	SIM 46	SIM 55	1.0	YES	YES	NO	STD	NO
G		SIM 8	SIM 23	SIM 47	SIM 54	1.0	YES	YES	YES	STD	NO
H		SIM 9	SIM 25	SIM 48	SIM 54	1.0	YES	YES	YES	6	NO
I		SIM 10	SIM 27	SIM 50	SIM 56	1.0	YES	YES	YES	6	YES

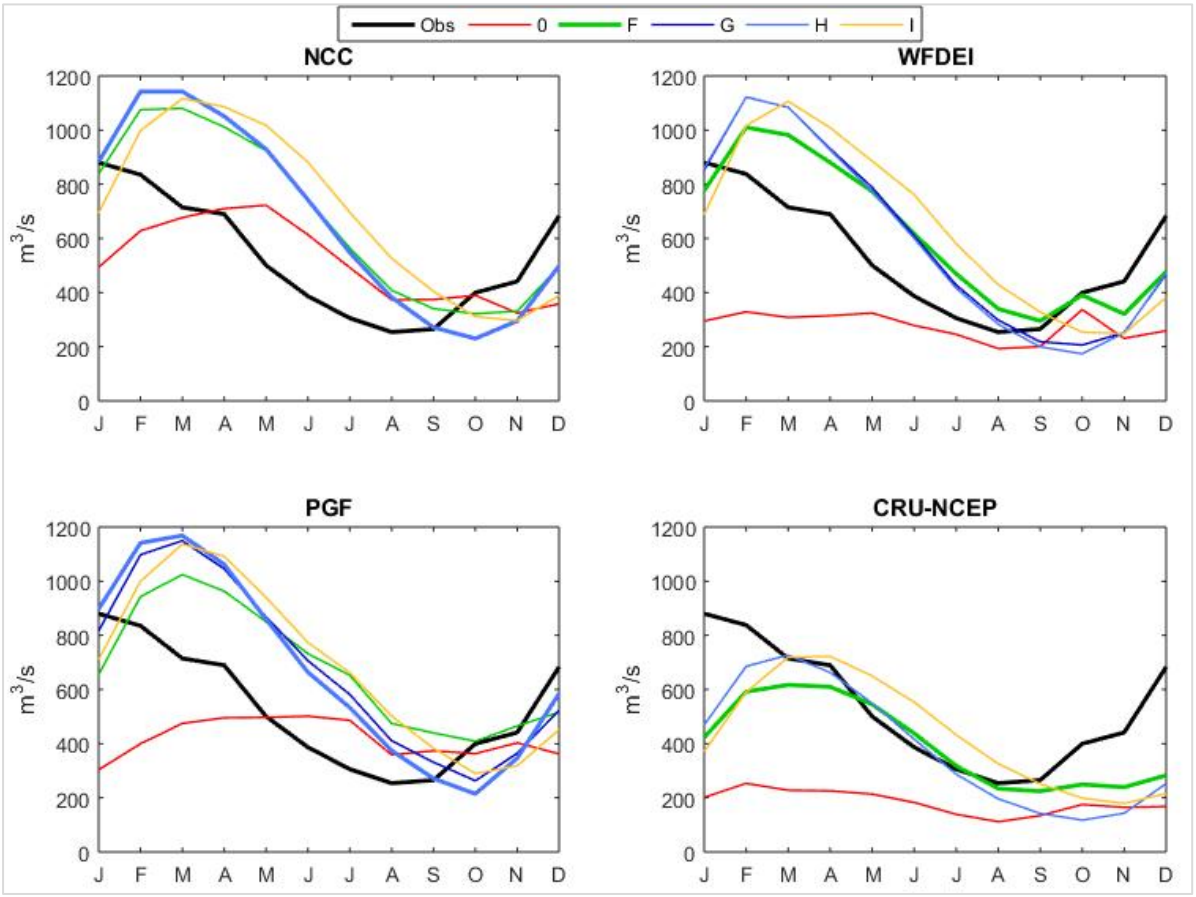

Figure 17. Pluriannual mean monthly average of discharge at Poses Station of final selection of simulations

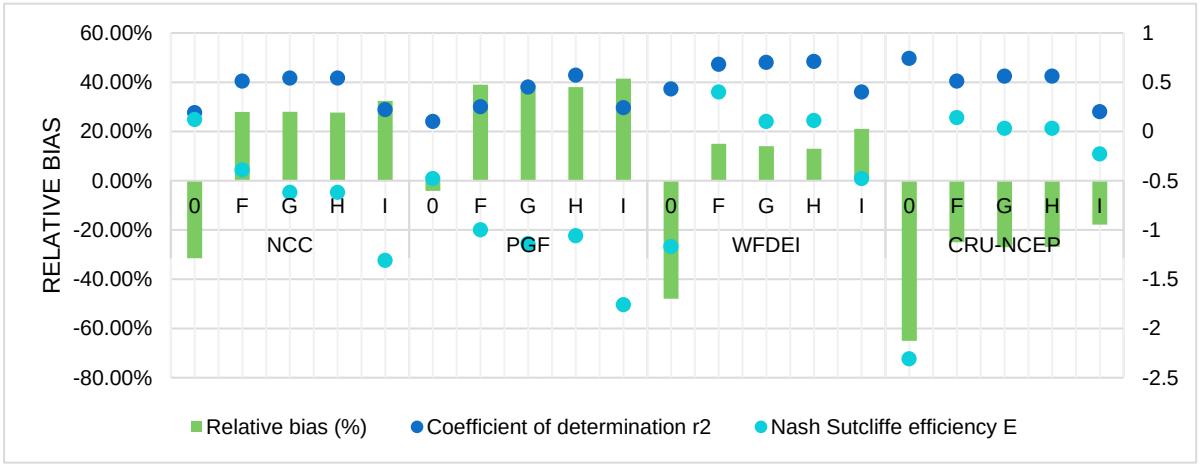

Figure 18. Performance criteria results for final selection of simulations

Table 5. Performance criteria for final selection of simulations – (Selected simulations shadowed in gray)

	NCC					PGF					WFDEI					CRU-NCEP				
	0	F	G	H	I	0	F	G	H	I	0	F	G	H	I	0	F	G	H	I
r^2	0,19	0,51	0,54	0,54	0,22	0,1	0,25	0,45	0,57	0,24	0,43	0,68	0,7	0,71	0,4	0,74	0,51	0,56	0,56	0,2
Nash Sutcliffe efficiency	0,12	-0,39	-0,62	-0,62	-1,31	-0,48	-1	-1,14	-1,06	-1,76	-1,17	0,4	0,1	0,11	-0,48	-2,31	0,14	0,03	0,03	-0,23
Relative bias (%)	-31,5	27,9	28,0	27,7	32,4	-4,1	39,0	39,0	38,0	41,5	-47,9	15,0	14,0	13,0	21,0	-65,0	-25,0	-27,0	-26,9	-17,8

The final simulation selection for each forcing are shadowed in grey in Table 5. This selection was based on different criteria, the volume of the final discharge, the seasonal behavior and the results of the efficiency criteria. The end result was based on the seasonality rather than the bias.

Figure 19 provides an overview of how well the simulation result fit the observation based on the minimum, maximum and mean yearly discharge over the 20 year period simulation. In the case of NCC, it shows a better simulation of the minimum discharges and of the highest ones. WFDEI shows in general better simulations, with less disperse results than any other forcing but still underestimating maximum values of discharge. PGF, on the contrary does not show a clear tendency, overestimating some values and underestimating others. CRU-NCEP, as expected, shows an overall underestimation of all the discharge values, but particularly for the maximum yearly means. If we compare it to Figure 9, we can see that the main improvements are seen over the WFDEI and CRU-NCEP forcing,

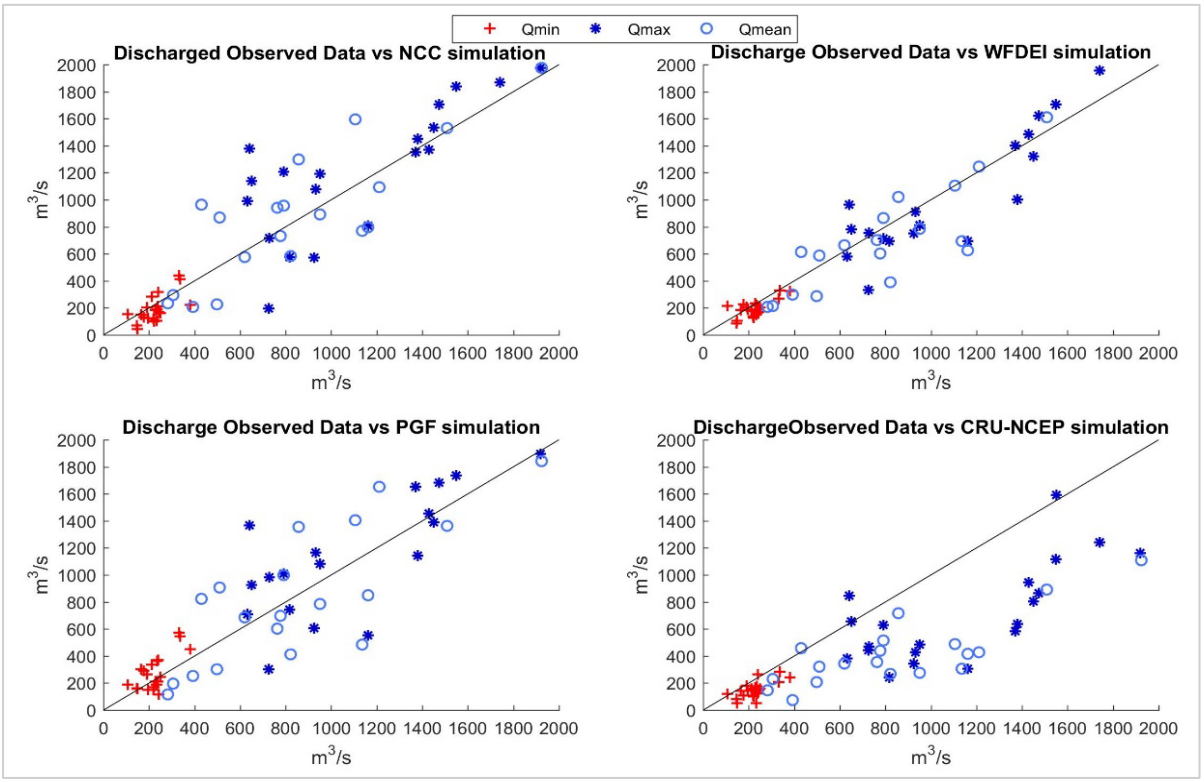

Figure 19. Comparison between observation (x-axis) and simulation discharge (y-axis), considering the annual mean of the maximum (Qmax), minimum (Qmin) and mean discharge (Qmean) for each of the 20 years (1981-2000) of study. Final selection of simulations

6. THE IMPACT OF WET AND DRY SEASONS

One of the questions that arouse during the study was related to possible effect of the dry and wet seasons and the models response. Under these considerations, the results were divided in two periods:

- Dry: Considering the years 1990, 1991 and 1992.
- Wet: Considering the years 1981, 1982 and 1983.

Figure 20 compares the results obtained with the final simulations (in grey in Table 5) over the two periods, with the corresponding performance criteria in
Figure *21*. WFDEI is the only forcing that presented better results for the dry period, however it showed a negative bias compared to the wet period. On the contrary, NCC and PGF forcings tend to have worse results during the dry years, showing an overestimation of the discharge during the months of March to August and an underestimation between the months of September to January which can be also be attributed to a lag between the total runoff and final discharge. This is explained by the evapotranspiration values over the same period. Since the seasonal variation of discharge for these forcing is not synchronized with the observations, both of them showed lower Nash values for the dry period. As for CRU-NCEP, the high values of total evapotranspiration and low precipitation adds to even a worse scenario for the dry period than the wet period.
Figure 23 shows a summary of the efficiency parameters for all the simulations performed with the latest trunk for all forcings. The results suggest that in general, there is a better response of the model over the wet years than over dry years.

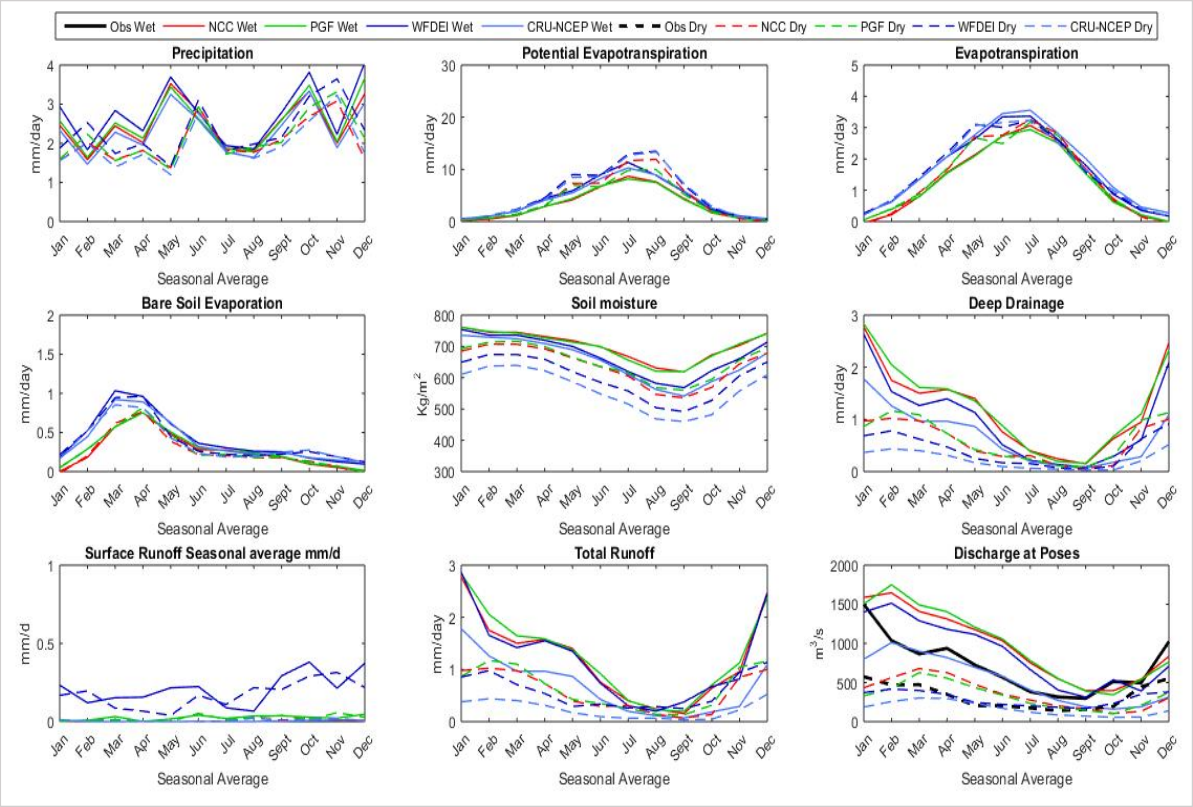

Figure 20. Final selection of simulations results for dry and wet periods

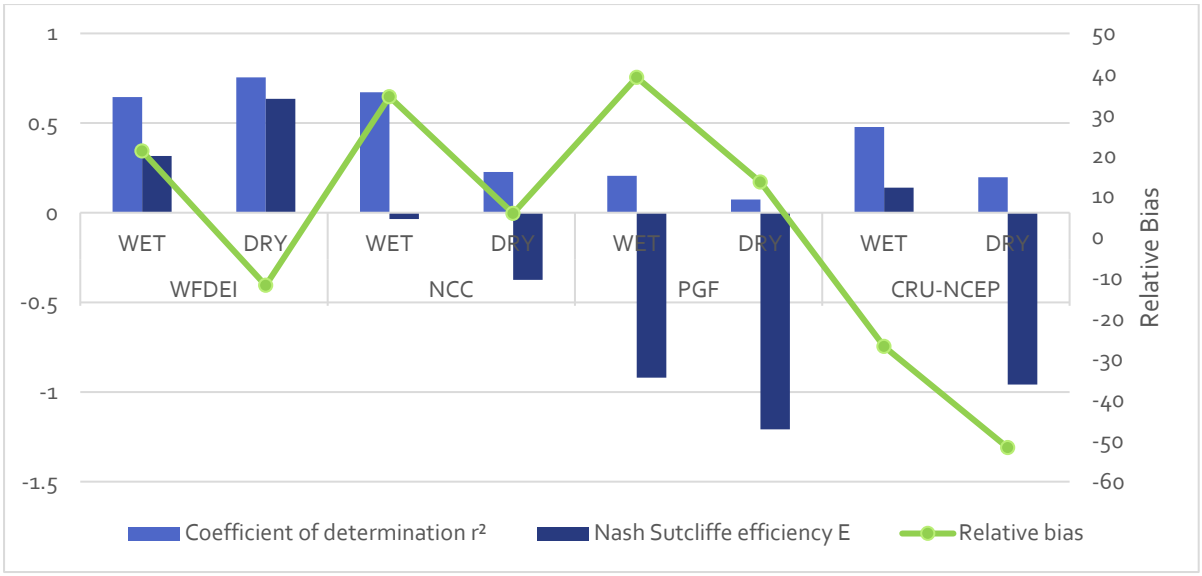

Figure 21. Wet and dry period results for performance criteria parameters.

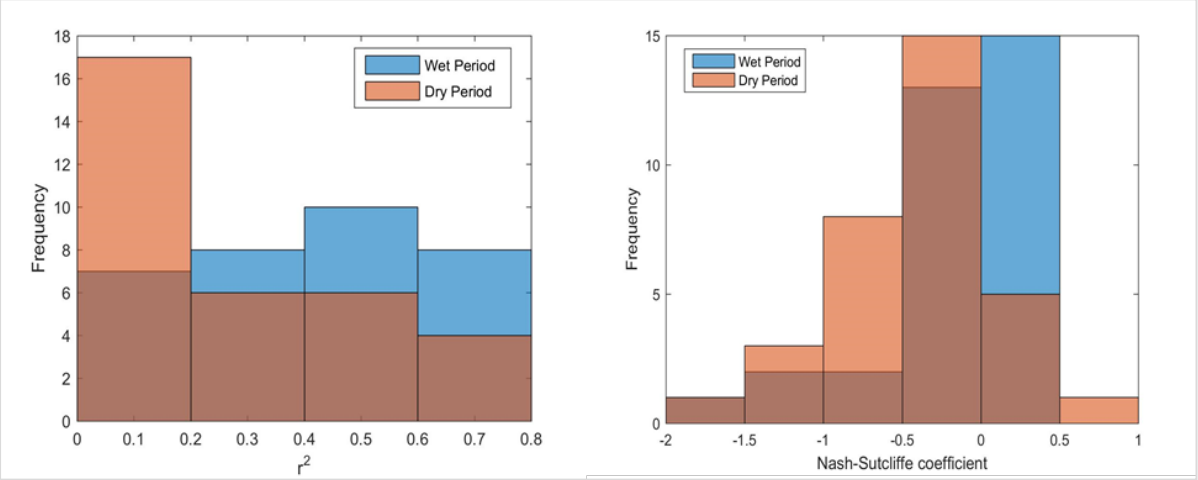

Figure 22. Distribution for the Coefficient of determination and Nash Sutcliffe coefficient for Wet and Dry periods for a total of 33 simulations all of them which included de corrected water stress modification.

V. CONCLUSIONS

In this study we used the Land Surface Model ORCHIDEE in “off line” mode to simulate the water and energy budgets of the Seine basin over a 22-year period, from 1979 to 2000. Initially we aimed to analyze the sensitivity of the model to the routing scheme of the streamflow, however, we identified that the model did not reproduce a reasonable water budget for the area of study which redirected our focus towards getting better results on this matter. In order to do this, we tested different options of the model that allowed us to work with different variables involved in the atmospheric-surface exchange. To evaluate our results we selected the river discharge at Poses station as a point of comparison between the simulations and the observation data.

Four forcing files were tested: NCC, PGF, WFDEI and CRU-NCEP. The sensitivity of the model to the forcing file was evident in regards of the total discharge produced showing that the NCC and PGF forcing produced considerably (almost 3 times) more river discharge than the WFDEI and CRU-NCEP. This is a response to the interaction of the atmospheric conditions given by the forcing file and that have an effect on the overall energy—water budget. Moreover, the results also suggested that the forcings overestimated certain variables in the water budget such as the surface runoff, which was the case of the PGF forcing. This had an effect over the partitioning between drainage and surface runoff therefore resulting in very different soil water equilibrium states and simulated discharge. More importantly, the results showed that there is a lag between the simulated discharge and the observations. This can be attributed to the routing scheme and the way it is adjusted to model the stream flows over the river basin, however this was not addressed in our study and we believe it should be considered as a further topic of interest.

The modifications that were tested assessed two main process: the soil hydrology and the vegetation modeling. For the vegetation related parameters, the most effective changes were the activation of STOMATE and dynamic roughness and the modification of the extinction coefficient. The dynamic roughness had a reductive effect on the potential evapotranspiration contributing to a bigger discharge which was enhanced by the modification of the vegetation extinction coefficient. The result was similar for all the four forcings. On the other hand, the STOMATE module played a bigger role in the seasonality of the simulations due to the dynamic LAI which addresses the change in the vegetation phenology over time and therefore produces a more realistic scenario than a fixed LAI map.

In the case of the soil hydrology parameters, the results were less effective in increasing the levels of discharge however the goal was to reduce the surface runoff and increase the infiltration flux. The spread of the precipitation naturally showed an effect over the surface runoff by reducing it as the precipitation is more uniformly distributed over the forcing time step. Nonetheless, it was the modification of the sub grid infiltration that had a larger effect by increasing the drainage and reducing the surface runoff by considering a uniform infiltration over the whole column of soil.

Finally, the selection of final simulations was based on the most effective combinations of changes for each one of the forcings. We considered the bias and Nash values in order to assess this decision. In all of the cases we considered the activation of STOMATE, dynamic roughness and vegetation extinction coefficient since they were a multiplying factor of a discharge. For both, NCC and PGF, we considered the modification of the sub grid infiltration as an additional modification which lead to a better seasonality and improved the issue of the elevated surface runoff.

Concluding, we achieved the main goal of this study by improving the levels of river discharge for all of the forcings tested. In spite of this, the simulations did not showed the same seasonality as the observations which is explained by the lag between total runoff and discharge. This suggests that additional work on the routing scheme can improve these results. Moreover, the choice of forcing file may also require further validation tests such as the ones performed using the latent heat flux

BIBLIOGRAPHY

Billen, G. et al., 2009. *Le bassin de la Seine - Découvrir les fonctions et les services rendus par le système Seine*, Available at: http://www.sisyphe.upmc.fr/piren/?q=webfm_send/816.

Blyth, E. et al., 2010. Evaluating the JULES Land Surface Model Energy Fluxes Using FLUXNET Data. *Journal of Hydrometeorology*, 11(2), pp.509–519.

Bonan, G., 2006. Land Surface Models for Climate Models : Description and Application Role of land surface models in GCMs. , (June).

Campoy, A. et al., 2013. Response of land surface fluxes and precipitation to different soil bottom hydrological conditions in a general circulation model. , 118(October), pp.725–739.

Carsel, R.F. & Parrish, R.S., 1988. Developing joint probability distributions of soil water retention characteristics. *Water Resources Research*, 24(5), pp.755–769. Available at: http://doi.wiley.com/10.1029/WR024i005p00755 [Accessed August 23, 2016].

Decharme, B. & Douville, H., 2007. Global validation of the ISBA sub-grid hydrology. *Climate Dynamics*, 29(1), pp.21–37.

Decharme, B. & Douville, H., 2006. Uncertainties in the GSWP-2 precipitation forcing and their impacts on regional and global hydrological simulations. *Climate Dynamics*, 27(7-8), pp.695–713.

d'Orgeval, T. (2006). Impact du changement climatique sur le cycle de l'eau en Afrique de l'Ouest : Mod´elisation et incertitudes. PhD thesis, UPMC. 187 pp. d'Orgeval, T., Polcher, J., and de Rosnay, P. (2008). Sensitivity of the West African hydrological cycle in ORCHIDEE to infiltration processes. Hydrol. Earth Syst. Sci, 12:1387–1401.

Dingman, L., 2015. *Physical Hydrology* Third., New Hampshire.

Ducharne, A. et al., 2003. Development of a high resolution runoff routing model, calibration and application to assess runoff from the LMD GCM. *Journal of Hydrology*, 280(1-4), pp.207–228.

Ducharne, A. et al., 2007. Long term prospective of the Seine River system: Confronting climatic and direct anthropogenic changes. *Science of the Total Environment*, 375(1-3), pp.292–311.

Ducharne, A., 2015. *The hydrol module of ORCHIDEE: scientific documentation*,

Ducoudré, N.I., Laval, K. & Perrier, A., 1993. SECHIBA, a New Set of Parameterizations of the Hydrologic Exchanges at the Land-Atmosphere Interface within the LMD Atmospheric General Circulation Model. *Journal of Climate*, 6, pp.248–273.

Gao, X. et al., 2004. *An approach for remote sensing validation of land surface schemes on a global scale*,

Gascoin, S. et al., 2009. Adaptation of a catchment-based land surface model to the hydrogeological setting of the Somme River basin (France). *Journal of Hydrology*, 368(1-4), pp.105–116. Available at: http://dx.doi.org/10.1016/j.jhydrol.2009.01.039.

van Genuchten, M.T., 1980. A Closed-form Equation for Predicting the Hydraulic Conductivity of Unsaturated Soils1. *Soil Science Society of America Journal*, 44(5), p.892.

GIP Seine-Aval, 2013. Du bassin à la baie de Seine - Fiche thématique. , p.6 p.

Guimberteau, M. et al., 2009. Simulations of Mississippi river basin streamflows by the land surface model ORCHIDEE . Sensitivity to the forcing resolution and parameters .

Guimberteau, M. et al., 2014. Testing conceptual and physically based soil hydrology schemes against observations for the Amazon Basin. *Geoscientific Model Development*, 7(3), pp.1115–1136.

Gupta, H. V. et al., 2009. Decomposition of the mean squared error and NSE performance criteria: Implications for improving hydrological modelling. *Journal of Hydrology*, 377(1), pp.80–91.

Haughton, N. et al., 2016. The plumbing of land surface models: is poor performance a result of methodology or data quality? *Journal of Hydrometeorology*, pp.JHM–D–15–0171.1. Available at: http://journals.ametsoc.org/doi/abs/10.1175/JHM-D-15-0171.1?af=R.

Hurkmans, R.T.W.L. et al., 2008. Water balance versus land surface model in the simulation of Rhine river discharges. *Water Resources Research*, 44(1), pp.1–14.

Krause, P. & Boyle, D.P., 2005. Comparison of different efficiency criteria for hydrological model assessment. *Advances In Geosciences*, pp.89–97.

Krinner, G. et al., 2005. A dynamic global vegetation model for studies of the coupled atmosphere-biosphere system. , 19.

Krinner, G. et al., 2005. A dynamic global vegetation model for studies of the coupled atmosphere-biosphere system. *Global Biogeochemical Cycles*, 19(1), pp.1–33.

Manabe, S., 1969. Climate and the Ocean Circulation 1. *Monthly Weather Review*, 97(11), pp.739–774. Available at: http://journals.ametsoc.org/doi/abs/10.1175/1520-0493(1969)097<0739:CATOC>2.3.CO;2.

Marengo, J.A. et al., 1994. Calculations of river-runoff in the GISS GGM: impact of a new land-surface parameterization and runoff routing model on the hydrology of the Amazon River. *Climate Dynamics*, 10(6-7), pp.349–361.

Materia, S. et al., 2010. The Sensitivity of Simulated River Discharge to Land Surface Representation and Meteorological Forcings. *Journal of Hydrometeorology*, 11(2), pp.334–351.

Mualem, Y., 1976. A new model for predicting the hydraulic conductivity of unsaturated porous media. *Water Resources Research*, 12(3), pp.513–522. Available at: http://doi.wiley.com/10.1029/WR012i003p00513 [Accessed August 23, 2016].

Ngo-Duc, T. et al., 2007a. Validation of the land water storage simulated by Organising Carbon and Hydrology in Dynamic Ecosystems (ORCHIDEE) with Gravity Recovery and Climate Experiment (GRACE) data. *Water Resources Research*, 43(4).

Ngo-Duc, T. et al., 2007b. Validation of the land water storage simulated by Organising Carbon and Hydrology in Dynamic Ecosystems (ORCHIDEE) with Gravity Recovery and Climate Experiment (GRACE) data. *Water Resources Research*, 43(4), pp.1–8.

Ngo-Duc, T., Polcher, J. & Laval, K., 2005. A 53-year forcing data set for land surface models. *Journal of Geophysical Research D: Atmospheres*, 110(6), pp.1–13.

Overgaard, J., Rosbjerg, D. & Butts, M.B., 2005. Land-surface modelling in hydrological perspective. *Biogeosciences Discussions*, 2(6), pp.1815–1848.

Pitman, A.J., 2003. The evolution of, and revolution in, land surface schemes designed for climate models. *International Journal of Climatology*, 23(5), pp.479–510.

Richards, L.A., 1931. Capillary conduction of liquids through porous mediums. *Journal of Applied Physics*, 1(5), pp.318–333.

Rosnay, P. De & Polcher, J., 2002. Impact of a physically based soil water flow and soil-plant interaction representation for modeling large-scale land surface processes. , 107(2).

Rousset, F. et al., 2004. Hydrometeorological modeling of the Seine basin using the SAFRAN-ISBA-MODCOU system. *Journal of Geophysical Research D: Atmospheres*, 109(14), pp.1–20.

Seine-Normady Water Agency, 2002. *PILOT CASE STUDIES: A FOCUS ON REAL-WORLD EXAMPLES*, Available at: http://webworld.unesco.org/water/wwap/case_studies/seine_normandy/.

Sheffield, J., Goteti, G. & Wood, E.F., 2006. Development of a 50-year high-resolution global dataset of meteorological forcings for land surface modeling. *Journal of Climate*, 19(13), pp.3088–3111.

Sitch, S. et al., 2003. Evaluation of ecosystem dynamics, plant geography and terrestrial carbon cycling in the LPJ dynamic global vegetation model. *Global Change Biology*, 9(2), pp.161–185. Available at: http://doi.wiley.com/10.1046/j.1365-2486.2003.00569.x [Accessed August 23, 2016].

Su, Z. et al., 2001. An Evaluation of Two Models for Estimation of the Roughness Height for Heat Transfer between the Land Surface and the Atmosphere. *Journal of Applied Meteorology*, 40(11), pp.1933–1951.

Tootchi, A., 2015. Toward a better representation of Soil evaporation in ORCHIDEE model : state and pathways of improvement. , 2(September).

U.S. Department of the Interior & Survey, U.S.G., 2016. The water cycle. Available at: http://water.usgs.gov/edu/watercycle.html.

University of Illinois, The Earth's Water Budget. *WW2010 Project*. Available at: http://ww2010.atmos.uiuc.edu/(Gl)/guides/mtr/hyd/bdgt.rxml.

Viennot, P. et al., 2009. *Hydrogéologie du bassin de la Seine : Comprendre et anticiper le fonctionnement hydrodynamique du bassin pour une gestion durable de la ressource*,

Vorosmarty, C.J. et al., 2000. Global system of rivers: Its role in organizing continental land mass and defining land-To-Ocean linkages. *Global Biogeochemical Cycles*, 14(2), pp.599–621.

Weedon, G.P. et al., 2014. Data methodology applied to ERA-Interim reanalysis data. *Water Resources Research*, 50(9), pp.7505–7514.

ANNEXE 1 – SUMMARY TABLE OF SIMULATIONS PERFORMED

SIMULATION	FORCING SOURCE	MODIFICATION IN THE CODE			SOIL HYDROLOGY PARAMETERS							VEGETATION RELATED PARAMETERES			
					VAN GENUTCHEN PARAMETERS				SATURATED HYDRAULIC CONDUCTIVITY		PRECIPITATION SPREAD				
		CORRECTED WATER STRESS	MODIFIED SUBGRID INFITLRATION	UNIFORM Ks	A0	A_POWER	N0	N_POWER	Ks_FACT	Ks_DECAY_RATE		STOMATE MODULE	LAI MAP	VEGETATION EXTINCTION COEFFICIENT	DYNAMIQUE ROUGHNESS
1	**NCC**	FALSE	FALSE	FALSE	0,00012*	0,53*	0,95*	0,34*	10*	2*	6	FALSE	STANDARD	0,5	FALSE
2	**NCC**	TRUE	FALSE	FALSE	0,00012	0,53	0,95	0,34	10	2	6	FALSE	STANDARD	0,5	FALSE
3	**NCC**	TRUE	FALSE	FALSE	0,00012	0,53	0,95	0,34	10	2	1	FALSE	ALTERNATIVE	0,5	FALSE
4	**NCC**	TRUE	FALSE	FALSE	0,00012	0,53	0,95	0,34	10	2	6	FALSE	STANDARD	1	FALSE
5	**NCC**	TRUE	FALSE	FALSE	0,00012	0,53	0,95	0,34	10	2	6	FALSE	STANDARD	0,5	TRUE
6	**NCC**	TRUE	FALSE	FALSE	0,00012	0,53	0,95	0,34	10	2	6	FALSE	STANDARD	1	TRUE
7	**NCC**	TRUE	FALSE	FALSE	0,00012	0,53	0,95	0,34	10	2	6	TRUE	-	1	TRUE
8	**NCC**	TRUE	TRUE	FALSE	0,00012	0,53	0,95	0,34	10	2	6	TRUE	-	1	TRUE
9	**NCC**	TRUE	FALSE	FALSE	0,00012	0,53	0,95	0,34	10	2	6	TRUE	-	1	TRUE
10	**NCC**	TRUE	TRUE	FALSE	0	0	0	0	20	1	6	TRUE	-	1	TRUE
11	**PGF**	FALSE	FALSE	FALSE	0,00012	0,53	0,95	0,34	10	2	3	FALSE	STANDARD	0,5	FALSE
12	**PGF**	FALSE	FALSE	FALSE	0,00012	0,53	0,95	0,34	10	2	3	FALSE	ALTERNATIVE	0,5	FALSE
13	**PGF**	TRUE	FALSE	FALSE	0,00012	0,53	0,95	0,34	10	2	3	FALSE	STANDARD	0,5	FALSE
14	**PGF**	TRUE	FALSE	FALSE	0,00012	0,53	0,95	0,34	10	2	3	FALSE	ALTERNATIVE	0,5	FALSE
15	**PGF**	TRUE	FALSE	FALSE	0,00012	0,53	0,95	0,34	10	2	1	FALSE	ALTERNATIVE	0,5	FALSE
16	**PGF**	TRUE	FALSE	FALSE	0,00012	0,53	0,95	0,34	10	2	6	FALSE	ALTERNATIVE	0,5	FALSE
17	**PGF**	TRUE	FALSE	FALSE	0,00012	0,53	0,95	0,34	10	2	3	FALSE	STANDARD	1	FALSE
18	**PGF**	TRUE	FALSE	FALSE	0,00012	0,53	0,95	0,34	10	2	3	FALSE	STANDARD	0,5	TRUE
19	**PGF**	TRUE	FALSE	FALSE	0,00012	0,53	0,95	0,34	10	2	3	FALSE	STANDARD	1	TRUE
20	**PGF**	TRUE	FALSE	FALSE	0,00012	0,53	0,95	0,34	10	2	6	FALSE	STANDARD	0,5	TRUE
21	**PGF**	TRUE	FALSE	FALSE	0,00012	0,53	0,95	0,34	10	2	3	TRUE	-	1	TRUE
22	**PGF**	TRUE	FALSE	FALSE	0,00012	0,53	0,95	0,34	10	2	3	TRUE	-	0,5	FALSE
23	**PGF**	TRUE	TRUE	FALSE	0,00012	0,53	0,95	0,34	10	2	3	TRUE	-	1	TRUE
24	**PGF**	TRUE	FALSE	FALSE	0,00012	0,53	0,95	0,34	10	2	6	TRUE	-	1	TRUE
25	**PGF**	TRUE	TRUE	FALSE	0,00012	0,53	0,95	0,34	10	2	6	TRUE	-	1	TRUE
26	**PGF**	TRUE	TRUE	FALSE	0	0	0	0	20	1	3	TRUE	-	1	TRUE

* Default values

SIMULATION	FORCING SOURCE	MODIFICATION IN THE CODE			SOIL HYDROLOGY PARAMETERS							VEGETATION RELATED PARAMETERES			
					VAN GENUTCHEN PARAMETERS				SATURATED HYDRAULIC CONDUCTIVITY		PRECIPITATION SPREAD				
		CORRECTED WATER STRESS	MODIFIED SUBGRID INFITLRATION	UNIFORM Ks	A0	A_POWER	N0	N_POWER	Ks_FACT	Ks_DECAY_RATE		STOMATE MODULE	LAI MAP	VEGETATION EXTINCTION COEFFICIENT	DYNAMIQUE ROUGHNESS
27	**PGF**	TRUE	TRUE	FALSE	0	0	0	0	20	1	6	TRUE	-	1	TRUE
28	**WFDEI**	FALSE	FALSE	FALSE	0,00012	0,53	0,95	0,34	10	2	3	FALSE	STANDARD	0,5	FALSE
29	**WFDEI**	FALSE	FALSE	FALSE	0,00012	0,53	0,95	0,34	20	2	3	FALSE	STANDARD	0,5	FALSE
30	**WFDEI**	FALSE	FALSE	FALSE	0,00012	0,53	0,95	0,34	20	1	3	FALSE	STANDARD	0,5	FALSE
31	**WFDEI**	FALSE	FALSE	FALSE	0,00012	0,53	0,95	0,34	20	4	3	FALSE	STANDARD	0,5	FALSE
32	**WFDEI**	FALSE	FALSE	FALSE	0	0	0	0	10	2	3	FALSE	STANDARD	0,5	FALSE
33	**WFDEI**	FALSE	FALSE	FALSE	0,00012	0,53	0,95	0,34	10	2	6	FALSE	STANDARD	0,5	FALSE
34	**WFDEI**	FALSE	FALSE	FALSE	0,00012	0,53	0,95	0,34	10	2	1	FALSE	STANDARD	0,5	FALSE
35	**WFDEI**	FALSE	TRUE	FALSE	0,00012	0,53	0,95	0,34	10	2	3	FALSE	STANDARD	0,5	FALSE
36	**WFDEI**	FALSE	TRUE	TRUE	0,00012	0,53	0,95	0,34	10	2	3	FALSE	STANDARD	0,5	FALSE
37	**WFDEI**	FALSE	TRUE	FALSE	0	0	0	0	20	1	3	FALSE	STANDARD	0,5	FALSE
38	**WFDEI**	TRUE	FALSE	FALSE	0,00012	0,53	0,95	0,34	10	2	3	FALSE	STANDARD	0,5	FALSE
39	**WFDEI**	TRUE	FALSE	FALSE	0,00012	0,53	0,95	0,34	10	2	3	FALSE	STANDARD	1	FALSE
40	**WFDEI**	TRUE	FALSE	FALSE	0,00012	0,53	0,95	0,34	10	2	3	FALSE	STANDARD	0,5	TRUE
41	**WFDEI**	TRUE	FALSE	FALSE	0,00012	0,53	0,95	0,34	10	2	3	FALSE	STANDARD	1	TRUE
42	**WFDEI**	TRUE	FALSE	FALSE	0,00012	0,53	0,95	0,34	10	2	6	FALSE	STANDARD	1	FALSE
43	**WFDEI**	TRUE	TRUE	FALSE	0	0	0	0	20	1	3	FALSE	STANDARD	1	FALSE
44	**WFDEI**	TRUE	TRUE	FALSE	0	0	0	0	20	1	3	FALSE	STANDARD	1	TRUE
45	**WFDEI**	TRUE	FALSE	FALSE	0,00012	0,53	0,95	0,34	10	2	3	TRUE	-	1	FALSE
46	**WFDEI**	TRUE	FALSE	FALSE	0,00012	0,53	0,95	0,34	10	2	3	TRUE	-	1	TRUE
47	**WFDEI**	TRUE	TRUE	FALSE	0,00012	0,53	0,95	0,34	10	2	3	TRUE	-	1	TRUE
48	**WFDEI**	TRUE	TRUE	FALSE	0,00012	0,53	0,95	0,34	10	2	6	TRUE	-	1	TRUE
49	**WFDEI**	TRUE	TRUE	FALSE	0	0	0	0	20	1	3	TRUE	-	1	TRUE
50	**WFDEI**	TRUE	TRUE	FALSE	0	0	0	0	20	1	6	TRUE	-	1	TRUE
51	**CRU-NCEP**	TRUE	FALSE	FALSE	0,00012	0,53	0,95	0,34	10	2	6	FALSE	STANDARD	1	FALSE
52	**CRU-NCEP**	TRUE	FALSE	FALSE	0,00012	0,53	0,95	0,34	10	2	6	FALSE	STANDARD	0,5	TRUE
53	**CRU-NCEP**	TRUE	FALSE	FALSE	0,00012	0,53	0,95	0,34	10	2	6	FALSE	STANDARD	1	TRUE
54	**CRU-NCEP**	TRUE	TRUE	FALSE	0,00012	0,53	0,95	0,34	10	2	6	TRUE	-	1	TRUE
55	**CRU-NCEP**	TRUE	FALSE	FALSE	0,00012	0,53	0,95	0,34	10	2	6	TRUE	-	1	TRUE
56	**CRU-NCEP**	TRUE	TRUE	FALSE	0	0	0	0	20	1	6	TRUE	-	1	TRUE

N.b.: The simulations shadowed in grey represent the final selection.

ANNEXE 2 – VALUES OF ANALYZED VARIABLES FOR EACH SIMULATION

VARIABLE	Air humidity	Wind speed	Net radiation	Precipitation	Potential evapotranspiration	Evapotranspiration	Bare soil evaporation	Transpiration	Evaporation from Canopy	Mean Leaf Area Index	"Total Soil Moisture"	"Deep drainage	Infiltration	Surface runoff	"Total Runoff"	Drainage/Total runoff	Discharge (Poses Station)
UNITS	g/g	m/s	W/m^2	mm/d	mm/d	mm/d	mm/d	mm/d	mm/day	"-"	Kg/m^2	mm/d	mm/d	mm/d	mm/d	(%)	M^3/s
1	0,00733	2,019	56,10	2,28	7,07	1,64	0,59	0,90	n/a	2,79	607,99	0,50	1,82	0,13	0,63	79,52%	438,52
2	0,00733	1,964	56,95	2,28	8,00	1,47	0,37	0,91	0,20	3,25	529,48	0,19	1,48	0,61	0,81	24,00%	585,84
3	0,00733	1,964	56,95	2,28	8,00	1,47	0,37	0,91	0,20	3,25	529,48	0,19	1,48	0,61	0,81	24,00%	585,84
4	0,00733	1,989	56,28	2,28	8,98	1,48	0,39	0,88	0,23	2,79	630,78	0,53	1,77	0,27	0,79	66,22%	561,41
5	0,00733	2,018	54,67	2,28	3,93	1,43	0,45	0,81	0,17	2,79	640,34	0,57	1,82	0,27	0,85	67,62%	589,33
6	0,00733	2,078	56,00	2,28	3,86	1,37	0,25	0,86	0,26	2,42	673,58	0,90	1,99	0,01	0,91	99,34%	656,51
7	0,00733	2,079	55,99	2,28	3,88	1,37	0,25	0,86	0,26	2,41	665,39	0,79	1,87	0,13	0,91	86,15%	658,33
8	0,00733	2,078	56,00	2,28	3,86	1,37	0,25	0,86	0,26	2,42	673,58	0,90	1,99	0,01	0,91	99,34%	656,51
9	0,00733	2,078	56,00	2,28	3,86	1,37	0,25	0,86	0,26	2,42	673,58	0,90	1,99	0,01	0,91	99,34%	656,51
10	0,00733	2,081	55,89	2,28	4,05	1,33	0,24	0,84	0,26	2,35	555,21	0,94	1,99	0,01	0,95	99,38%	681,95
11	0,00722	1,970	53,49	2,37	6,98	1,70	0,68	0,83	0,17	2,79	563,66	0,30	1,75	0,37	0,67	44,37%	424,02
12	0,00722	1,916	54,73	2,37	7,30	1,71	0,52	0,96	0,21	3,25	554,46	0,28	1,73	0,37	0,65	43,44%	405,88
13	0,00722	1,970	53,40	2,37	7,11	1,67	0,69	0,79	0,17	2,79	588,09	0,32	1,75	0,37	0,70	46,58%	450,72
14	0,00722	1,916	54,64	2,37	7,42	1,68	0,53	0,93	0,21	3,25	583,01	0,31	1,73	0,37	0,68	45,53%	426,35
15	0,00722	1,916	54,20	2,37	8,02	1,52	0,48	0,85	0,17	3,25	469,39	0,10	1,41	0,76	0,86	11,25%	595,84
16	0,00722	1,916	54,76	2,37	7,27	1,73	0,54	0,92	0,25	3,25	611,68	0,43	1,83	0,20	0,64	68,18%	381,88
17	0,00722	1,941	53,54	2,37	8,93	1,57	0,48	0,86	0,21	2,79	615,11	0,43	1,72	0,37	0,80	53,67%	524,83
18	0,00722	1,975	52,44	2,37	3,56	1,41	0,47	0,80	0,13	2,79	639,59	0,57	1,82	0,38	0,96	59,87%	635,60
19	0,00722	1,975	51,97	2,37	3,54	1,29	0,28	0,85	0,15	2,79	658,55	0,69	1,81	0,39	1,07	64,10%	728,82
20	0,00722	1,975	52,53	2,37	3,49	1,43	0,48	0,78	0,16	2,79	656,14	0,73	1,94	0,21	0,94	77,41%	615,00
21	0,00722	2,040	53,45	2,37	3,61	1,31	0,27	0,89	0,15	2,44	656,98	0,69	1,83	0,37	1,05	65,11%	722,72
22	0,00722	2,031	55,09	2,37	8,60	1,61	0.53	0.86	0.20	2.39	595.40	0.40	1.75	0.35	0.75	52,91%	497.32
23	0,00722	2,038	53,46	2,37	3,58	1,32	0,27	0,89	0,15	2,45	677,77	0,94	2,10	0,10	1,05	90,15%	717,44
24	0,00722	2,039	53,53	2,37	3,56	1,33	0,27	0,87	0,19	2,45	670,74	0,84	1,95	0,20	1,04	80,67%	710,99
25	0,00722	2,038	53,52	2,37	3,55	1,33	0,27	0,87	0,19	2,46	681,93	1,02	2,13	0,02	1,04	97,85%	708,57
26	0,00722	2,041	53,40	2,37	3,70	1,29	0,26	0,87	0,15	2,38	557,70	0,98	2,10	0,10	1,08	90,51%	737,18
27	0,00722	2,041	53,48	2,37	3,67	1,30	0,26	0,85	0,18	2,39	562,65	1,05	2,13	0,02	1,07	97,96%	727,49
28	0,00660	2,011	58,61	2,55	10,33	2,13	0,83	1,03	n/a	2,77	512,28	0,25	1,94	0,20	0,45	54,68%	236,66

VARIABLE	Air humidity	Wind speed	Net radiation	Precipitation	Potential evapotranspiration	Evapotranspiration	Bare soil evaporation	Transpiration	Evaporation from Canopy	Mean Leaf Area Index	"Total Soil Moisture"	"Deep drainage	Infiltration	Surface runoff	"Total Runoff"	Drainage/Total runoff	Discharge (Poses Station)
UNITS	g/g	m/s	W/m^2	mm/d	mm/d	mm/d	mm/d	mm/d	mm/day	"-"	Kg/m^2	mm/d	mm/d	mm/d	mm/d	(%)	M^3/s
29	0,00660	2,011	58,63	2,55	10,30	2,14	0,84	1,07	n/a	2,77	526,70	0,24	1,94	0,20	0,44	53,95%	233,24
30	0,00660	2,011	58,51	2,55	10,49	2,09	0,80	0,90	n/a	2,77	482,78	0,28	1,94	0,20	0,49	58,21%	253,90
31	0,00660	2,011	58,69	2,55	10,19	2,17	0,86	1,01	n/a	2,77	535,65	0,21	1,94	0,20	0,42	50,97%	225,03
32	0,00660	2,011	58,41	2,58	10,65	2,06	0,79	0,97	0,28	2,77	451,27	0,32	1,94	0,20	0,52	60,89%	273,97
33	0,00660	2,011	58,73	2,58	10,17	2,18	0,85	1,00	0,32	2,77	535,38	0,31	1,90	0,10	0,40	75,81%	184,44
34	0,00660	2,011	58,17	2,58	11,02	1,96	0,77	0,95	0,24	2,77	427,00	0,11	1,78	0,52	0,63	17,65%	438,08
35	0,00660	2,011	58,73	2,55	10,11	2,18	0,86	1,01	n/a	2,77	552,30	0,37	2,11	0,03	0,39	92,85%	161,21
36	0,00660	2,011	58,75	2,55	10,09	2,19	0,86	1,01	n/a	2,77	556,74	0,38	2,13	0,01	0,39	98,28%	161,07
37	0,00660	2,011	58,47	2,58	10,54	2,08	0,80	0,99	0,28	2,77	463,50	0,47	2,12	0,03	0,49	94,30%	231,49
38	0,00660	2,011	58,48	2,58	10,53	2,09	0,84	0,95	0,28	2,77	551,31	0,29	1,94	0,20	0,49	58,27%	269,43
39	0,00660	1,979	58,45	2,58	13,07	2,00	0,58	1,05	0,36	2,77	580,84	0,37	1,90	0,20	0,58	64,72%	332,25
40	0,00660	1,978	58,12	2,58	5,03	1,77	0,58	0,95	0,23	2,77	625,81	0,59	2,05	0,21	0,81	73,44%	492,44
41	0,00660	1,978	57,58	2,58	4,82	1,64	0,35	1,01	0,27	2,77	647,06	0,72	2,04	0,22	0,94	77,02%	601,17
43	0,00660	1,979	58,31	2,58	13,35	1,94	0,55	1,01	0,36	2,77	503,02	0,61	2,08	0,03	0,64	95,60%	359,07
44	0,00660	1,978	57,39	2,58	5,08	1,58	0,32	0,98	0,27	2,77	543,55	0,97	2,23	0,03	1,00	97,08%	639,41
45	0,00660	2,162	60,16	2,58	11,24	2,00	0,72	0,97	0,30	2,15	572,00	0,39	1,97	0,18	0,58	68,16%	329,26
46	0,00660	2,115	58,90	2,58	4,77	1,65	0,39	0,99	0,26	2,26	646,24	0,74	2,08	0,19	0,93	79,28%	594,00
47	0,00660	2,114	58,91	2,58	4,73	1,66	0,39	1,00	0,26	2,28	658,14	0,90	2,25	0,02	0,92	97,83%	586,41
48	0,00660	1,978	57,67	2,58	4,77	1,66	0,35	0,99	0,31	2,77	653,82	0,82	2,08	0,11	0,93	88,57%	586,28
48	0,00660	2,115	58,99	2,58	4,72	1,67	0,39	0,98	0,29	2,27	657,65	0,91	2,19	0,00	0,91	99,68%	577,59
49	0,00660	2,122	58,77	2,58	4.99	1,60	0,39	0,95	0.25	2,17	543,22	0,97	2,26	0,02	0,99	98,00%	629,46
50	0,00660	2,123	58,85	2,58	4.98	1,61	0,39	0,93	0.29	2,17	542,91	0,97	2,19	0,00	0,98	99,72%	621,18
51	0,00659	1,935	60,38	2,18	11,74	1,95	0,55	0,94	0,45	2,79	489,74	0,13	1,46	0,11	0,23	54,85%	178,20
52	0,00659	1,959	60,34	2,18	4,94	1,76	0,56	0,91	0,28	2,79	577,31	0,30	1,65	0,12	0,42	71,77%	306,74
53	0,00659	1,959	60,05	2,18	4,69	1,65	0,34	0,98	0,34	2,79	606,63	0,40	1,65	0,12	0,52	77,00%	384,13
54	0,00659	2,072	61,52	2,18	4,56	1,68	0,36	0,99	0,33	2,37	617,29	0,49	1,77	0,00	0,50	99,03%	373,21
55	0,00659	2,072	61,52	2,18	4,56	1,68	0,36	0,99	0,33	2,37	617,29	0,49	1,77	0,00	0,50	99,03%	373,21
56	0,00659	2,082	61,41	2,18	4,84	1.61	0,37	0,93	0,32	2,22	506,43	0,56	1,78	0,00	0,56	99,16%	420,40

ANNEXE 3: MODIFICATIONS ON PARAMETERS RELATED TO VEGETATION

Detail of combinations considered for the analysis of the influence of the parameters related to vegetation. Each combination correspond to a simulation number depending on the forcing.

COMBINATION		NCC	PGF	WFDEI	CRU-NCEP	VEGETATION EXTINCTION COEFFICIENT	DYNAMIC ROUGHNESS	STOMATE MODULE
A		SIM 2	SIM 13	SIM 38	-	0.5	NO	NO
B		SIM 4	SIM 17	SIM 39	SIM 51	1.0	NO	NO
C		-	SIM 22	SIM 40	-	1.0	NO	YES
D		SIM 6	SIM 19	SIM 41	SIM 53	1.0	YES	NO
E		SIM 5	SIM 18	SIM 45	SIM 52	0.5	YES	NO
F		SIM 8	SIM 21	SIM 46	SIM 54	1.0	YES	YES

PGF FORCING

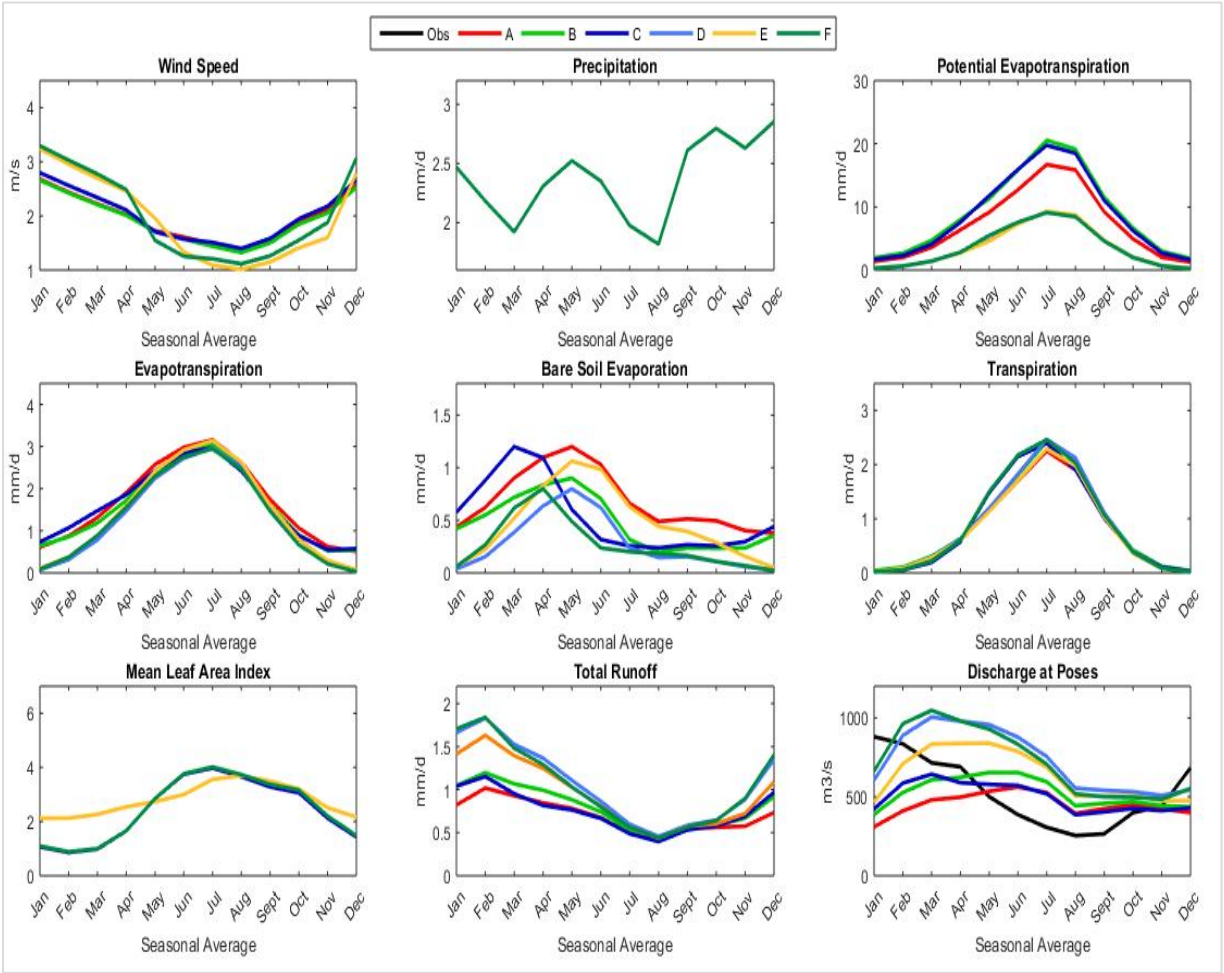

NCC FORCING

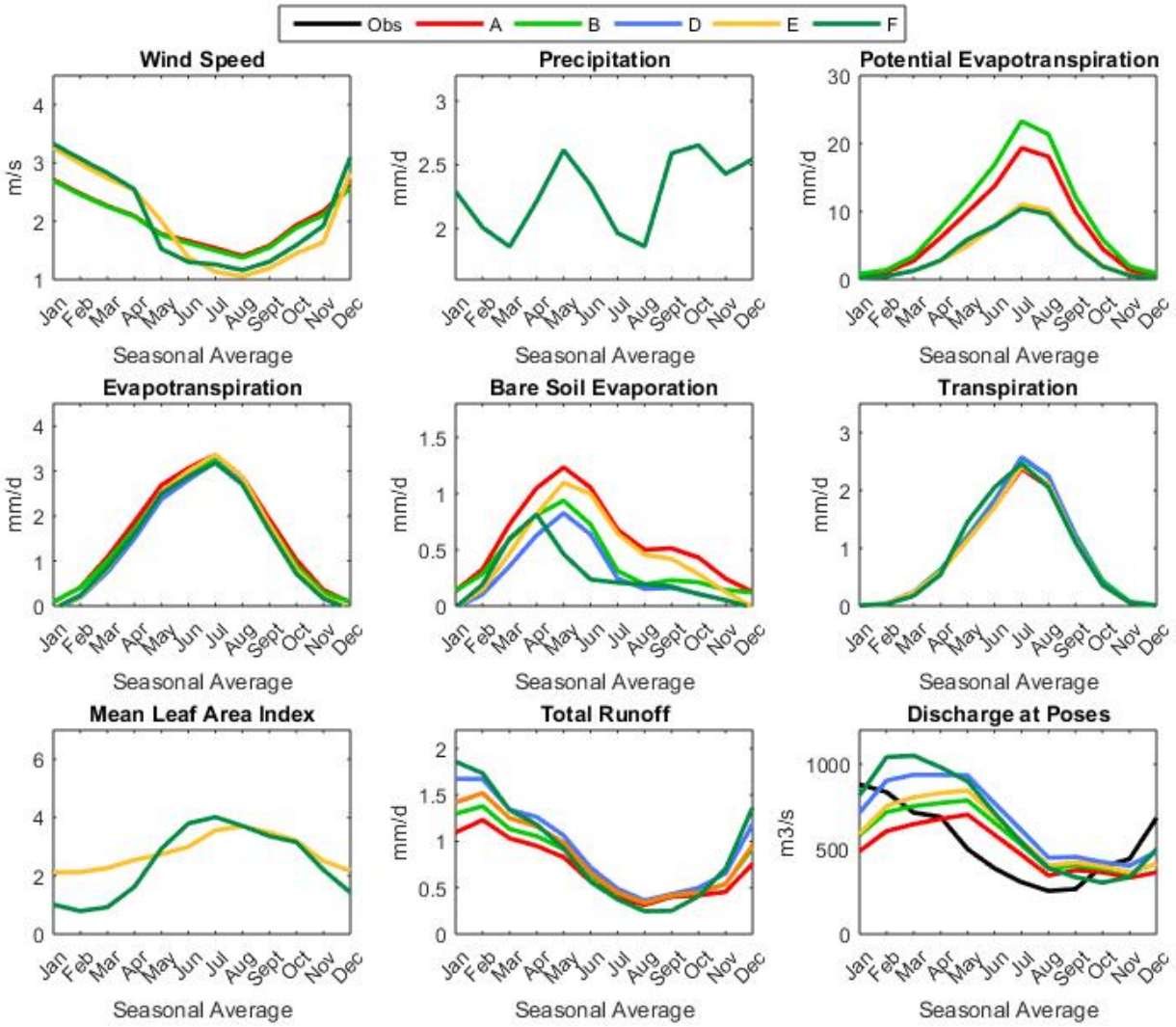
Obs
A
B
D
E
F
Wind Speed
m/s
Precipitation
mm/d
Potential Evapotranspiration
mm/d
Evapotranspiration
mm/d
Bare Soil Evaporation
mm/d
Transpiration
mm/d
Mean Leaf Area Index
Total Runoff
mm/d
Discharge at Poses
m3/s
Jan Feb Mar Apr May Jun Jul Aug Sept Oct Nov Dec
Seasonal Average

CRU-NCEP FORCING